Singularity formation in three-dimensional motion of a vortex sheet

By TAKASHI ISHIHARA† AND YUKIO KANEDA

Department of Applied Physics, Faculty of Engineering,
Nagoya University, Chikusa-ku, Nagoya 464-01, Japan

The evolution of a small but finite three-dimensional disturbance on a flat uniform vortex sheet is analysed on the basis of a Lagrangian representation of the motion. The sheet at time t is expanded in a double periodic Fourier series: $R(\lambda_1, \lambda_2, t) = (\lambda_1, \lambda_2, 0) + \sum_{n,m} A_{n,m} \exp[i(n\lambda_1 + \delta m\lambda_2)]$, where λ_1 and λ_2 are Lagrangian parameters in the streamwise and spanwise directions, respectively, and δ is the aspect ratio of the periodic domain of the disturbance. By generalizing Moore's analysis for two-dimensional motion to three dimensions, we derive evolution equations for the Fourier coefficients $A_{n,m}$. The behaviour of $A_{n,m}$ is investigated by both numerical integration of a set of truncated equations and a leading-order asymptotic analysis valid at large t. Both the numerical integration and the asymptotic analysis show that a singularity appears at a finite time $t_c = O(\ln \epsilon^{-1})$ where ϵ is the amplitude of the initial disturbance. The singularity is such that $A_{n,0} = O(t_c^{-1})$ behaves like $n^{-5/2}$, while $A_{n,\pm 1} = O(\epsilon t_c)$ behaves like $n^{-3/2}$ for large n. The evolution of $A_{0,m}$ (spanwise mode) is also studied by an asymptotic analysis valid at large t. The analysis shows that a singularity appears at a finite time $t = O(\epsilon^{-1})$ and the singularity is characterized by $A_{0,2k} \propto k^{-5/2}$ for large k.

1. Introduction

In many flows, vorticity is often confined to very thin surface-like regions. A vortex sheet is a basic model representing such a region and can be defined formally as a surface or interface across which the tangential component of the velocity field is discontinuous. It is well known that such an interface suffers an instability (Kelvin–Helmholtz instability) to streamwise disturbances, and the growth rate for an infinitesimal disturbance is inversely proportional to its streamwise wavelength (see e.g. Batchelor 1967). This instability causes the vortex sheet to roll up into various fascinating forms, but the analysis of such a roll-up process is known to be difficult particularly because of the strong nonlinearity of the self-induced motion of vortex sheet.

Regarding the two-dimensional motion of a vortex sheet, intensive studies have been made since the pioneering numerical study by Rosenhead (1931) (see Krasny 1990 and the references cited therein). However, most real flows are three-dimensional, and the dynamics in three dimensions is fundamentally different from that in two dimensions, particularly because of the existence of a vortex stretching mechanism

---

† Present address: Department of Mathematics, Faculty of Science, Toyama University, Gofuku, Toyama 930, Japan.

in three dimensions. In contrast to two-dimensional motion, very few studies have so far been made on three-dimensional motion, and little is known about the role of *three-dimensionality* or *vortex stretching* in the evolution of a vortex sheet. Recently a simple Lagrangian representation of the motion of a vortex sheet in three-dimensional flow has been derived by Caflisch (1989) and Kaneda (1990). The primary purpose of the present paper is to study analytically the nature of the three-dimensional motion of a vortex sheet on the basis of that representation.

Since our study on the three-dimensional motion of a vortex sheet is closely related to that on the two-dimensional one by Damms (unpublished; see Moore 1979) and Moore (1979), we briefly review their studies as a preliminary to studying the three-dimensional motion. In two-dimensional flow, a vortex sheet can be represented as a curve in the complex plane:

$$z(\lambda, t) = x(\lambda, t) + iy(\lambda, t),$$

where t is time and λ is a non-dimensional parameter. The motion of the vortex sheet is described by the Birkhoff–Rott equation (Birkhoff 1962; Rott 1956)

$$\frac{\partial z^*(\lambda, t)}{\partial t} = \frac{1}{2\pi i} \text{p.v.} \int_{-\infty}^{\infty} \frac{\gamma(\lambda')}{z(\lambda, t) - z(\lambda', t)} d\lambda', \tag{1.1}$$

where the asterisk denotes the complex conjugate and the symbol p.v. the principal value of the integral. The function $\gamma(\lambda)$ represents the circulation per unit λ. It is invariant along particle paths, and may be therefore regarded as a Lagrangian marker variable.

Damms (unpublished; see Moore 1979) studied the evolution of a vortex sheet subject to the initial condition

$$z(\lambda, 0) = \lambda + i\epsilon \sin \lambda, \quad \gamma(\lambda) = 1,$$

where $\epsilon \ll 1$. She expanded $z(\lambda, t)$ in a Fourier series as

$$z(\lambda, t) = \lambda + \sum_{n=-\infty}^{\infty} A_n(t) e^{in\lambda}. \tag{1.2}$$

Substituting (1.2) into (1.1) yields a set of ordinary differential equations for the coefficients $A_n(t)$, where each equation includes an infinite number of interactions among the Fourier modes. By assuming $|A_n(t)| = O(\epsilon^{|n|})$ and discarding terms of $O(\epsilon^{15})$, she derived a set of truncated equations and integrated numerically the equations. She showed that at a critical time $t_c = O(\ln(\epsilon^{-1}))$, the Fourier coefficient A_n decays with n at an algebraic rate n^p for large n, where the exponent p is about -2.5. This implies that the interface is smooth but the curvature diverges for some λ. The singularity characterized by $p = -2.5$ is, therefore, called two-dimensional curvature singularity.

In his analytical study, Moore (1979) used the following expansion of A_n:

$$A_n(t) = \epsilon^{|n|} A_n^{(0)}(t) + \epsilon^{|n|+2} A_n^{(2)}(t) + \cdots, \tag{1.3}$$

and divided the whole set of equations into simpler subsets for $A_n^{(0)}, A_n^{(2)}, \cdots$. The

equation for $A_n^{(0)} (n > 0)$ is

$$\frac{\mathrm{d}A_n^{(0)\bullet}}{\mathrm{d}t} = \frac{1}{2} \left[A_n^{(0)}(-\mathrm{i})n + \overset{(2)}{\sum} A_{n_1}^{(0)} A_{n_2}^{(0)}(-\mathrm{i})^2 n_1 n_2 + \cdots \right.$$
$$\left. + \overset{(K)}{\sum} A_{n_1}^{(0)} \cdots A_{n_K}^{(0)}(-\mathrm{i})^K n_1 \cdots n_K + \cdots + (A_1^{(0)})^n(-\mathrm{i})^n \right], \qquad (1.4)$$

where

$$\overset{(K)}{\sum} \equiv \begin{pmatrix} \text{sum with respect to} \quad n_1, \cdots, n_K, \\ \text{satisfying} \\ n_1 + n_2 + \cdots + n_K = n, \quad n_1, n_2, \cdots, n_K \geqslant 1 \end{pmatrix}.$$

Equation (1.4) is linear in $A_n^{(0)}$ and involves only $A_s^{(0)}$ satisfying $1 \leqslant s < n$. By analysing (1.4), he derived the following asymptotic expression for large n and t:

$$\epsilon^n A_n^{(0)}(t) \sim (2\pi)^{-1/2}(1+\mathrm{i})t^{-1}n^{-5/2} \exp[n(1 + \tfrac{1}{2}t + \ln\tfrac{1}{4}\epsilon t)].$$

This implies that at time t_c defined by

$$1 + \tfrac{1}{2}t_c + \ln\tfrac{1}{4}\epsilon t_c = 0, \qquad (1.5)$$

the nth Fourier coefficient decays with n like $n^{-5/2}$, instead of exponentially, and the analyticity of the sheet shape is therefore lost. These results are consistent with Damms'.

Meiron, Baker & Orszag (1982) examined the evolution of a vortex sheet subject to the initial condition

$$z(\lambda, 0) = \lambda, \quad \gamma(\lambda) = 1 + \epsilon \cos \lambda,$$

by using a Taylor series expansion in time. They also found that the sheet develops a singularity at $t \approx t_c$, in agreement with Moore (1979). Krasny (1986) studied the evolution of a vortex sheet subject to

$$z(\lambda, 0) = \lambda + (1 - \mathrm{i})\epsilon \sin \lambda, \quad \gamma(\lambda) = 1.$$

He applied the point vortex approximation to the Birkhoff–Rott equation and numerically followed the motion of the vortex sheet. He also obtained evidence for the appearance of a singularity in the shape of the vortex sheet. Shelley (1992) re-examined the same initial value problem as in Meiron *et al.* (1982) by applying a spectrally accurate approximation to the Birkhoff–Rott integral. He also obtained results consistent with Moore (1979) and also showed that for finite amplitude initial disturbance and near the singularity time, the form of singularity may depart away from the one predicted by Moore (1979).

It is seen from the derivation of Moore (1979) that his asymptotic analysis is verified only for the case of small but finite disturbance. However, as shown in Meiron *et al.* (1982), Krasny (1986) and Shelley (1992), his simple analysis gives a fairly good prediction of the appearance time as well as the form and the location of a singularity even for the case of finite disturbance. For two dimensions, knowledge of singularity formation in the shape of a vortex sheet plays an important role in understanding the intrinsic nature of a vortex sheet.

In this paper, as a first step to understanding the nature of the three-dimensional motion of a vortex sheet, we extend the above numerical and analytical studies by Damms and Moore, respectively, to three-dimensional motion on the basis of a

Lagrangian representation of the three-dimensional motion of a vortex sheet. Let the initial shape of a vortex sheet be given by

$$R(\lambda_1, \lambda_2, 0) = (\lambda_1, \lambda_2, 0) + (\epsilon_2 \sin \delta \lambda_2, 0, \epsilon_1 \sin \lambda_1), \tag{1.6}$$

where $\delta \equiv a/b$ is the aspect ratio with a and b being the streamwise and the spanwise wavelength of the initial disturbance, respectively. The flow is two-dimensional if $\epsilon_2 = 0$, as assumed by Damms and Moore. If $\epsilon_1 = 0$, the vortex sheet is flat but each vortex line is distorted on the flat sheet. In order to make the problem analytically tractable, we confine ourselves to the case of small but finite ϵ_2, and assume

$$0 < \epsilon_1 \ll 1 \quad \text{and} \quad \epsilon_2 = O(\epsilon_1). \tag{1.7}$$

In spite of the smallness of the disturbance, the analysis still retains some of the genuine three-dimensional and nonlinear nature of the vortex sheet evolution.

As a straightforward generalization of (1.2) to three dimensions, the vortex sheet at time t is represented in a Fourier series as

$$R(\lambda_1, \lambda_2, t) = (\lambda_1, \lambda_2, 0) + \sum_{n,m} A_{n,m}(t) \exp[\mathrm{i}(n\lambda_1 + \delta m\lambda_2)].$$

The equations governing the evolution of $A_{n,m}(t)$ will be derived in §2. A truncation method used by Damms (see Moore 1979) is applied to the set of equations governing $\{A_{n,m}(t)\}$, and the truncated set thus obtained is integrated numerically in §3. The numerical solutions suggest that, at a critical time $t_c = O(\ln\epsilon_1^{-1})$, the Fourier coefficients $A_{n,0}$ and $A_{n,\pm 1}$ decay with n algebraically for large n.

The truncated set of equations presented in §3 is intractably nonlinear, and inconvenient for analytical derivation of the asymptotic nature of the Fourier coefficient for large n and m. It is therefore interesting to derive a simpler set. Such a set can be obtained by expanding each Fourier coefficient in powers of ϵ_1 and ϵ_2 and retaining only the leading-order terms in the expansion, which is an extension of (1.3) to three dimensions. A brief report on an asymptotic analysis on the basis of this expansion has been made by Ishihara & Kaneda (1994). It was shown that at a finite time $t_c = O(\ln\epsilon_1^{-1})$, the Fourier coefficient $A_{n,0}$ behaves like $n^{-2.5}$ for large n, while $A_{n,\pm 1}$ behaves like $n^{-1.5}$. In §4 we present the above analysis in a complete form and derive analytically the leading-order asymptotic form of $A_{n,\pm 1}$ for the case of small δ. For $A_{n,0}$, the form will be seen to be equivalent to that obtained by Moore (1979). In §5, we study the evolution of the spanwise mode $A_{0,m}$ on the basis of the simpler set derived in §4. Discussion and conclusions are presented in §6. We also consider in §6 the sheet shape near the singularity time and present a few interpretations of the results obtained in §4.

2. Basic equations

Let us consider an infinitely thin vortex sheet in an ideal incompressible fluid of unit density that obeys

$$\frac{\partial u}{\partial t} + (u \cdot \nabla)u = -\nabla p, \tag{2.1}$$

$$\nabla \cdot u = 0, \tag{2.2}$$

where u and p are the velocity and the pressure of the fluid, respectively. If the vorticity is confined to the vortex sheet, then there exists a velocity potential $\phi = \phi(r, t)$ such that $u = \nabla\phi$ outside the sheet, where r denotes the position vector. Let the position

vector r of a point on the vortex sheet S at time t be represented by two parameters λ_1 and λ_2 as

$$r(t) = R(\lambda_1, \lambda_2, t),$$

and let $\Phi(\lambda_1, \lambda_2, t)$ be the jump of the velocity potential across S at time t defined by

$$\Phi(\lambda_1, \lambda_2, t) \equiv \phi^+[R(\lambda_1, \lambda_2, t), t] - \phi^-[R(\lambda_1, \lambda_2, t), t],$$

where

$$\phi^\pm(r, t) \equiv \lim_{\epsilon \to 0} \phi(r \pm \epsilon n, t), \quad n \equiv \frac{N}{|N|}, \quad N \equiv \frac{\partial R}{\partial \lambda_1} \times \frac{\partial R}{\partial \lambda_2}.$$

Then, the motion of S is given by

$$\frac{\partial R(\lambda_1, \lambda_2, t)}{\partial t} = V[R(\lambda_1, \lambda_2, t)], \tag{2.3}$$

where

$$V(r) = -\frac{1}{4\pi} \text{p.v.} \int\int_S \frac{X \times W(\lambda_1', \lambda_2', t)}{|X|^3} d\lambda_1' d\lambda_2' + u_H,$$

$$X \equiv r - R(\lambda_1', \lambda_2', t),$$

$$W(\lambda_1, \lambda_2, t) = \frac{\partial \Phi(\lambda_1, \lambda_2, t)}{\partial \lambda_1} \frac{\partial R(\lambda_1, \lambda_2, t)}{\partial \lambda_2} - \frac{\partial \Phi(\lambda_1, \lambda_2, t)}{\partial \lambda_2} \frac{\partial R(\lambda_1, \lambda_2, t)}{\partial \lambda_1},$$

and the vector u_H represents the contribution from the irrotational flow field. The fluid density is continuous across the sheet under consideration, and Φ is therefore shown to be time-independent under the dynamics given by (2.1) and (2.2) (Caflisch 1989; Kaneda 1990). When there is a density discontinuity across the interface, Φ may be time-dependent as in the case studied by Baker, Meiron, & Orszag (1984).

If the parameters λ_1 and λ_2 are so chosen that W is parallel to $\partial R/\partial \lambda_2$ at $t = 0$, then $\partial \Phi/\partial \lambda_2 = 0$, i.e. $\partial \Phi/\partial \lambda_1$ is a function of only λ_1. Then we may write W as

$$W(\lambda_1, \lambda_2, t) = \gamma(\lambda_1) \frac{\partial R(\lambda_1, \lambda_2, t)}{\partial \lambda_2}. \tag{2.4}$$

The vorticity density Ω on the sheet is given by

$$\Omega(\lambda_1, \lambda_2, t) \equiv n \times (\nabla\phi^+ - \nabla\phi^-)$$
$$= \left| \frac{\partial R(\lambda_1, \lambda_2, t)}{\partial \lambda_1} \times \frac{\partial R(\lambda_1, \lambda_2, t)}{\partial \lambda_2} \right|^{-1} W, \tag{2.5}$$

and is related to the vorticity ω as

$$\Omega = \int \omega \, dn, \tag{2.6}$$

where $\Omega \cdot n = 0$, n is the distance along the sheet normal n. When W is given by (2.4), we call the line given by $\lambda_1 =$ constant a vortex line. This vortex line is parallel to Ω, and the strength $\gamma(\lambda_1)$ is a Lagrangian invariant and constant along the vortex line.

In equation (2.3), the vortex stretching may be represented in terms of W. Consider a small parallelepiped with two opposite faces which lie on either side of the vortex sheet and which are parallel to the vortex sheet. Suppose that the two faces are a sufficiently small distance h apart at $t = 0$ and have area corresponding to the increments $\Delta\lambda_1$ and $\Delta\lambda_2$ in the Lagrangian coordinates. Then the volume of the small

parallelepiped at $t = 0$ is given by

$$\Delta V = h \left| \frac{\partial \mathbf{R}}{\partial \lambda_1} \times \frac{\partial \mathbf{R}}{\partial \lambda_2} \right| \Delta \lambda_1 \Delta \lambda_2. \tag{2.7}$$

From the incompressibility condition (2.2), ΔV is a constant along the particle path. Let $\bar{\omega}$ be the averaged value of the vorticity defined by

$$\bar{\omega} \equiv \frac{1}{h} \int \omega \mathrm{d}n. \tag{2.8}$$

Then it can be shown from (2.5)–(2.8) that

$$W = \frac{\Delta V}{\Delta \lambda_1 \Delta \lambda_2} \bar{\omega} \propto \bar{\omega},$$

and the variation of W therefore reflects vortex stretching.

Now let us consider a flat and uniform infinite vortex sheet lying in the (x, y)-plane, on each side of which the velocity is uniform and given by

$$\mathbf{u}(x, y, z) = \begin{cases} (\frac{1}{2}U, 0, 0), & z > 0, \\ (-\frac{1}{2}U, 0, 0), & z < 0. \end{cases}$$

The sheet may be represented parametrically as

$$\mathbf{R}(\lambda_1, \lambda_2) = \frac{\gamma_0}{U} \begin{pmatrix} \lambda_1 \\ \lambda_2 \\ 0 \end{pmatrix}, \tag{2.9}$$

where γ_0 and U are constants and related to the circulation function Γ as $\mathrm{d}\Gamma \equiv U\mathrm{d}x = \gamma_0 \mathrm{d}\lambda_1$, and λ_1 and λ_2 are dimensionless parameters in the streamwise (x) and spanwise (y) directions, respectively.

Suppose that vortex sheet (2.9) is slightly deformed initially both in the streamwise and spanwise directions as

$$\mathbf{R}(\lambda_1, \lambda_2, 0) = \frac{\gamma_0}{U} \left[\begin{pmatrix} \lambda_1 \\ \lambda_2 \\ 0 \end{pmatrix} + \begin{pmatrix} \epsilon_2 \sin[2\pi(\lambda_2 + \psi_2)/b] \\ 0 \\ \epsilon_1 \sin[2\pi(\lambda_1 + \psi_1)/a] \end{pmatrix} \right], \tag{2.10}$$

where a and b are the streamwise and the spanwise wavelength of the initial disturbance, respectively, and ψ_1 and ψ_2 can be set to be zero without loss of generality.

Introducing non-dimensional variables defined by $\lambda_1 = (a/2\pi)\hat{\lambda}_1$, $\lambda_2 = (a/2\pi)\hat{\lambda}_2$, $t = (a\gamma_0/2\pi U^2)\hat{t}$, and

$$\mathbf{R}(\lambda_1, \lambda_2, t) = \frac{a\gamma_0}{2\pi U} \hat{\mathbf{R}}(\hat{\lambda}_1, \hat{\lambda}_2, \hat{t}),$$

we may write (2.3) in the following dimensionless form:

$$\frac{\partial}{\partial \hat{t}} \hat{\mathbf{R}}(\hat{\lambda}_1, \hat{\lambda}_2, \hat{t}) = -\frac{1}{4\pi} \text{p.v.} \int \int_S \frac{\hat{\mathbf{X}} \times \hat{\mathbf{W}}(\hat{\lambda}_1', \hat{\lambda}_2', \hat{t})}{|\hat{\mathbf{X}}|^3} \mathrm{d}\hat{\lambda}_1' \mathrm{d}\hat{\lambda}_2', \tag{2.11}$$

where $\hat{\mathbf{X}} \equiv \mathbf{X}/(a\gamma_0/2\pi U)$, $\hat{\mathbf{W}} \equiv \mathbf{W}/(a\gamma_0^2/2\pi U) = \partial \hat{\mathbf{R}}(\hat{\lambda}_1', \hat{\lambda}_2', \hat{t})/\partial \hat{\lambda}_2'$, and we have assumed $\mathbf{u}_H = 0$. Similarly (2.10) with $\psi_1 = \psi_2 = 0$ may be written as

$$\hat{\mathbf{R}}(\hat{\lambda}_1, \hat{\lambda}_2, 0) = \begin{pmatrix} \hat{\lambda}_1 \\ \hat{\lambda}_2 \\ 0 \end{pmatrix} + \begin{pmatrix} \hat{\epsilon}_2 \sin \delta \hat{\lambda}_2 \\ 0 \\ \hat{\epsilon}_1 \sin \hat{\lambda}_1 \end{pmatrix}, \tag{2.12}$$

where $\hat\epsilon_1 = \epsilon_1/(a/2\pi)$, $\hat\epsilon_2 = \epsilon_2/(a/2\pi)$, and δ is the aspect ratio a/b of the periodic domain of the initial disturbance. Hereafter, we shall omit the hats for simplicity.

Since (2.11) is compatible with the periodicity of $R - (\lambda_1, \lambda_2, 0)$ in λ_1 and λ_2, we may expand $R(\lambda_1, \lambda_2, t)$ in a Fourier series as

$$R(\lambda_1, \lambda_2, t) = \begin{pmatrix} \lambda_1 \\ \lambda_2 \\ 0 \end{pmatrix} + \sum_{n,m} A_{n,m}(t) e^{i(n\lambda_1 + \delta m\lambda_2)}, \qquad (2.13)$$

in which

$$A_{n,m}(t) \equiv \begin{pmatrix} X_{n,m}(t) \\ Y_{n,m}(t) \\ Z_{n,m}(t) \end{pmatrix}.$$

Since initial condition (2.12) satisfies the antisymmetry $R(-\lambda_1, -\lambda_2) = -R(\lambda_1, \lambda_2)$ and equation (2.11) is compatible with this symmetry, the Fourier coefficient satisfies $A_{-n,-m}(t) = -A_{n,m}(t)$. This implies that $A_{n,m}$ is pure imaginary.

Because of (2.12), the Fourier coefficients $A_{n,m}$ satisfy the initial conditions

$$\left.\begin{aligned} X_{0,1}(0) &= -X_{0,-1}(0) = -\tfrac{1}{2}\epsilon_2 i, \\ Z_{1,0}(0) &= -Z_{-1,0}(0) = -\tfrac{1}{2}\epsilon_1 i, \\ X_{n,m}(0) &= Y_{n,m}(0) = Z_{n,m}(0) = 0, \quad \text{otherwise.} \end{aligned}\right\} \qquad (2.14)$$

Equations governing the evolution of the Fourier coefficients $A_{n,m}$ are obtained by substituting (2.13) into (2.11).

In the following we put $\lambda_1' = \lambda_1 + \alpha$ and $\lambda_2' = \lambda_2 + \beta$, so that (2.13) gives

$$X = R(\lambda_1, \lambda_2, t) - R(\lambda_1', \lambda_2', t) = \begin{pmatrix} -\alpha \\ -\beta \\ 0 \end{pmatrix} + \begin{pmatrix} s_x \\ s_y \\ s_z \end{pmatrix}, \qquad (2.15)$$

and

$$W = \frac{\partial}{\partial \lambda_2'} R(\lambda_1', \lambda_2', t) = \begin{pmatrix} 0 \\ 1 \\ 0 \end{pmatrix} + \begin{pmatrix} s_{2x} \\ s_{2y} \\ s_{2z} \end{pmatrix}, \qquad (2.16)$$

where

$$\begin{pmatrix} s_x \\ s_y \\ s_z \end{pmatrix} \equiv \sum_{n,m} \begin{pmatrix} X_{n,m}(t) \\ Y_{n,m}(t) \\ Z_{n,m}(t) \end{pmatrix} (1 - e^{i(n\alpha + \delta m\beta)}) e^{i(n\lambda_1 + \delta m\lambda_2)}, \qquad (2.17a)$$

$$\begin{pmatrix} s_{2x} \\ s_{2y} \\ s_{2z} \end{pmatrix} \equiv \sum_{n,m} i\delta m \begin{pmatrix} X_{n,m}(t) \\ Y_{n,m}(t) \\ Z_{n,m}(t) \end{pmatrix} e^{i(n\alpha + \delta m\beta)} e^{i(n\lambda_1 + \delta m\lambda_2)}. \qquad (2.17b)$$

From (2.15), we have

$$|X|^{-3} = (\alpha^2 + \beta^2)^{-3/2} (1 - 2S_1 + S_2)^{-3/2}, \qquad (2.18)$$

in which

$$S_1 \equiv \frac{\alpha s_x + \beta s_y}{\alpha^2 + \beta^2}, \quad S_2 \equiv \frac{s_x^2 + s_y^2 + s_z^2}{\alpha^2 + \beta^2}.$$

Substituting (2.15), (2.16) and (2.18) into (2.11) gives

$$\sum_{n,m} \frac{\mathrm{d}}{\mathrm{d}t} \begin{pmatrix} X_{n,m} \\ Y_{n,m} \\ Z_{n,m} \end{pmatrix} e^{\mathrm{i}(n\lambda_1 + \delta m\lambda_2)} = -\frac{1}{4\pi} \mathrm{p.v.} \int_{-\infty}^{\infty} \int_{-\infty}^{\infty} \frac{\mathrm{d}\alpha\, \mathrm{d}\beta}{(\alpha^2 + \beta^2)^{3/2}}$$

$$\times \begin{pmatrix} -s_z - \beta s_{2z} + s_y s_{2z} - s_z s_{2y} \\ \alpha s_{2z} + s_z s_{2x} - s_x s_{2z} \\ -\alpha + s_x - \alpha s_{2y} + \beta s_{2x} + s_x s_{2y} - s_y s_{2x} \end{pmatrix} \times (1 - 2S_1 + S_2)^{-3/2}. \quad (2.19)$$

Let $\epsilon = \max(\epsilon_1, \epsilon_2) \ll 1$. Because of initial condition (2.14), we assume that $A_{n,m} = O(\epsilon)$ and therefore

$$S_1 = O(\epsilon), \quad S_2 = O(\epsilon^2). \quad (2.20)$$

This assumption is the same in spirit as the one used by Moore (1979), who showed the validity of assumption (2.20) in the two-dimensional case. Under the assumption (2.20), we can expand $|X|^{-3}$ and therefore the integrand in (2.19) in powers of ϵ. Equating the coefficients of $\exp[\mathrm{i}(n\lambda_1 + \delta m\lambda_2)]$ then yields the governing equation for $A_{n,m} \equiv (X_{n,m}, Y_{n,m}, Z_{n,m})$ in the following form:

$$\frac{\mathrm{d}}{\mathrm{d}t} A_{n,m} = LA_{n,m} + P, \quad (2.21)$$

where L is evaluated to be

$$L \equiv \frac{1}{2} \begin{pmatrix} 0 & 0 & n^2(n^2 + \delta^2 m^2)^{-1/2} \\ 0 & 0 & \delta nm(n^2 + \delta^2 m^2)^{-1/2} \\ (n^2 + \delta^2 m^2)^{1/2} & 0 & 0 \end{pmatrix}, \quad (2.22)$$

and P is expressed, in a symbolic notation, as

$$P \equiv \sum_{\{n,m\}}^{(2)} \{A\}^2 + \cdots + \sum_{\{n,m\}}^{(K)} \{A\}^K + \cdots, \quad (2.23)$$

in which

$$\sum_{\{n,m\}}^{(K)} \equiv \begin{pmatrix} \text{sum with respect to} \quad n_1, \cdots, n_K, m_1, \cdots, m_K, \\ \text{satisfying} \\ n_1 + n_2 + \cdots + n_K = n \;\; m_1 + m_2 + \cdots + m_K = m \end{pmatrix}, \quad (2.24)$$

and $\{A\}^{(K)}$ indicates terms of degree K in $A_{p,q}$.†

In (2.23) each element of the vector P contains an infinite series of products of the Fourier modes $A_{p,q}$, and the coefficient of each product is in general of the form,

$$G = \mathrm{p.v.} \int_0^{2\pi} \mathrm{d}\theta \int_0^{\infty} \mathrm{d}R \cos^j \theta \sin^k \theta \frac{g^{(i)}(R, \theta)}{R^{i+1}}, \quad (2.25)$$

where

$$\mathrm{p.v.} \int_0^{2\pi} \mathrm{d}\theta \int_0^{\infty} \mathrm{d}R \equiv \lim_{\epsilon \to 0} \int_0^{2\pi} \mathrm{d}\theta \int_\epsilon^{\infty} \mathrm{d}R,$$

i, j and k are certain positive integers satisfying $i + j + k =$ odd number, and

† A copy of pages giving the algebraic details is available on request from either the authors or the JFM Editorial Office.

$$g^{(i)}(R, \theta) = \{1 - \exp iR(n_1 \cos \theta + \delta m_1 \sin \theta)\} \cdots$$
$$\times \{1 - \exp iR(n_i \cos \theta + \delta m_i \sin \theta)\}, \tag{2.26}$$

where $(n_1, m_1), \cdots, (n_i, m_i)$ stand for interacting wavenumbers.

Since the evaluation of integrals of type (2.25) plays a key role in writing down the equations for the evolution of $A_{n,m}$, we briefly describe how to evaluate G. By repeating the partial integrations with respect to R and noting $i+j+k$ =odd number, it is shown that

$$G = \frac{1}{i!} \text{p.v.} \int_0^{2\pi} d\theta \int_0^\infty dR \cos^j \theta \sin^k \theta \frac{1}{R} \left(\frac{\partial}{\partial R} \right)^i g^{(i)}(R, \theta). \tag{2.27}$$

Thus the evaluation of G can be reduced to that of integrals of the form

$$I = \frac{1}{i!} \text{p.v.} \int_0^{2\pi} d\theta \int_0^\infty dR \cos^j \theta \sin^k \theta \frac{1}{R} \left(\frac{\partial}{\partial R} \right)^i \exp\{iR(n \cos \theta + \delta m \sin \theta)\}.$$

Since

$$\exp\{iR(n \cos \theta + \delta m \sin \theta)\} = \exp\{iRa \sin(\theta + \Pi)\}$$
$$= \sum_{\mu=-\infty}^\infty J_\mu(Ra) \exp\{i\mu(\theta + \Pi)\},$$

I is expressed as

$$I = \frac{1}{i!} \text{p.v.} \int_0^{2\pi} d\theta \int_0^\infty dR \cos^j \theta \sin^k \theta \sum_{\mu=-\infty}^\infty \exp\{i\mu(\theta + \Pi)\} \frac{1}{R} \left(\frac{d}{dR} \right)^i J_\mu(Ra),$$

where

$$a = (n^2 + \delta^2 m^2)^{1/2}, \quad \exp\{i\Pi\} = \delta m/a + in/a,$$

and J_μ is a Bessel function of the first kind. Using $dJ_\mu(R)/dR = (1/2)\{J_{\mu-1}(R) - J_{\mu+1}(R)\}$ repeatedly, we have

$$\left(\frac{d}{dR} \right)^i J_\mu(Ra) = \left(\frac{a}{2} \right)^i \sum_{l=0}^i (-1)^l \binom{i}{l} J_{\mu-i+2l}(Ra)$$

and therefore

$$I = \frac{1}{i!} \left(\frac{a}{2} \right)^i \text{p.v.} \int_0^{2\pi} d\theta \int_0^\infty dz \cos^j \theta \sin^k \theta$$
$$\times \sum_{\mu=-\infty}^\infty \exp\{i\mu(\theta + \Pi)\} \sum_{l=0}^i (-1)^l \binom{i}{l} \frac{J_{\mu-i+2l}(z)}{z},$$

where $\binom{i}{l}$ is the Binomial coefficient and we have put $z = Ra$. When $\mu = i - 2l$, the integrand diverges at $z = 0$. In order to evaluate the principal value of the integral, we need to estimate the following integral with respect to θ:

$$c(\mu) \equiv \int_0^{2\pi} \cos^j \theta \sin^k \theta e^{i\mu\theta} d\theta. \tag{2.28}$$

It can be readily seen that if $j + k + \mu$ is an odd number or if $|\mu| > j + k$, $c(\mu)$ is equal to zero. Since $i + j + k - 2l$ is an odd number as well as $i + j + k$, $c(i - 2l) = 0$ and therefore the principal value is equal to zero when $\mu = i - 2l$. In addition, $c(\mu)$ is non-zero only if μ is every other integer from $-(j + k)$ to $j + k$ and for such values of μ, $(\mu - i + 2l)$ is an odd number. Noting this fact and using the recursive relations among the Bessel functions, and

$$J_{-n}(z) = (-1)^n J_n(z), \qquad \int_0^\infty J_n(z)\mathrm{d}z = 1,$$

for positive integer n, we have

$$\int_0^\infty \mathrm{d}z \frac{J_{\mu-i+2l}(z)}{z} = \frac{1}{\mu - i + 2l}.$$

Consequently, we have

$$I = \frac{1}{i!}\left(\frac{a}{2}\right)^i \sum_{\mu=-(j+k)}^{j+k} c(\mu) \exp\{i\mu\Pi\} \sum_{l=0}^i (-1)^l \binom{i}{l} \frac{1}{\mu - i + 2l}. \tag{2.29}$$

It is rather straightforward to write down the explicit form of (2.23) by using the above evaluation. However the equations are quite lengthy and we omit here writing them in order to save space.†

3. Numerical integration of the truncated equations

From the conditions (2.14) and (2.20), the dominant term in P is initially proportional to $Z_{1,0}^n X_{0,1}^m = O(\epsilon_1^{|n|} \epsilon_2^{|m|})$. This suggests that

$$A_{n,m} = O(\epsilon_1^{|n|} \epsilon_2^{|m|}), \tag{3.1}$$

for $t = O(1)$.

A tempting way to simplify (2.21) is therefore to truncate the equations by discarding terms of order less than a certain order, say ϵ_1^M, where M is an appropriate integer. The evolution equations can be then reduced to $3 \times n_M$ ordinary differential equations for the $3 \times n_M$ Fourier coefficients $\{X_{p,q}, Y_{p,q}, Z_{p,q}\}$, where n_M is the number of pairs of integers $\{(p,q)\}$ such that $|p| + (\ln\epsilon_2/\ln\epsilon_1)|q| \leq M$.

For the sake of simplicity, we put $\delta \equiv a/b = 1$ and $\epsilon_1 = \epsilon_2 (\equiv \epsilon)$ throughout this section. The truncated set therefore consists of a set of ordinary differential equations for the Fourier coefficients $\{X_{p,q}, Y_{p,q}, Z_{p,q}\}$, where p and q are integers satisfying $|p| + |q| \leq M$, and retains only terms whose order is greater than or equal to ϵ^M. Because of the symmetry condition $A_{-n,-m}(t) = -A_{n,m}(t)$, the number of the equations can be reduced to $3M(M + 1)$.

Since the number of the terms on the right-hand side of the truncated equations increases in proportion to $M!$, it is out of question to treat the equations only by hand. We therefore used the algebraic manipulation language *Mathematica* on a SUN Spark Station 2. The process of the construction of the truncated equations can be divided roughly into two steps. First, we make a list of all possible interactions.

† A copy of pages giving the equations and the related algebraic details is available on request from either the authors or the JFM Editorial Office.
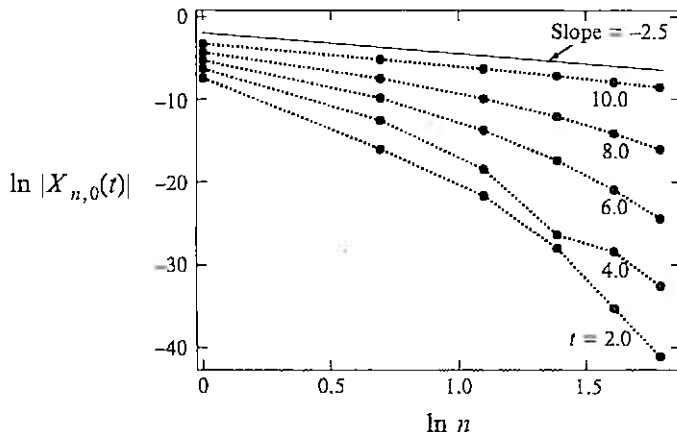
FIGURE 1. A plot of $\ln|X_{n,0}(t)|$ *vs.* $\ln n$ at times $t = 2.0, 4.0, 6.0, 8.0, 10.0$, showing the behaviour of the numerical solution of the truncated set in the case $\epsilon_1 = \epsilon_2 = 0.001$. The thin straight line has slope -2.5.

Second, we evaluate integral coefficients for each interaction.† It proved possible to work with M as large as 6 and the truncated set with $M = 6$ has about 7×10^4 terms.

In order to determine the singularity in the shape of vortex sheet in three-dimensional flow, we need to know the asymptotic behaviour of the Fourier coefficients $A_{n,m}$ for large n and m. However, as mentioned above, the number of terms to be treated increases so rapidly with M that the manageable magnitude of M, i.e. $|n| + |m|$, is quite limited in actual computation ($|n| + |m| \leqslant 6$ in our computation). It is therefore fair to regard the results obtained here only as suggestive regarding the asymptotic behaviour for large n and m.

The truncated equations with initial condition (2.14) were integrated numerically using the fourth-order Runge–Kutta method. In the run reported below, we set $\epsilon = 0.001$ and $\Delta t = 0.01$.

Figure 1 shows the n-dependence of streamwise Fourier coefficient $X_{n,0}$ at $t = 2.0$, 4.0, 6.0, 8.0, 10.0. It suggests that, for $t < 10$, the Fourier coefficient $X_{n,0}$ decays exponentially with respect to n, but, at $t \approx 10.0$, it decays only algebraically like $n^{-\alpha}$ with $\alpha \approx 2.5$. Fourier coefficient $Z_{n,0}$ behaves in the same way (not plotted here). This behaviour suggests that the sum

$$\sum_{n=-\infty}^{\infty} A_{n,0} \exp[i(n\lambda_1)] \tag{3.2}$$

loses analyticity at $t \approx 10.0$.

In the two-dimensional case (no spanwise disturbances, i.e. $\epsilon_2 = 0$), Moore (1979) showed analytically that the singularity time t_c is given by (1.5) and at $t = t_c$ the Fourier coefficient A_n of the disturbance behaves like $n^{-5/2}$ for large n. For $\epsilon_1 = 0.001$, (1.5) gives $t_c \approx 9.986$. The singularity time t_c and the behaviour of $A_{n,0}$ at $t \approx t_c$ are thus in good agreement with Moore's two-dimensional analysis. These facts suggest that the behaviour of $A_{n,0}$ is mainly determined by the two-dimensional dynamics of the vortex sheet provided that the amplitude of disturbance is sufficiently small.

Figure 2 shows the n-dependence of $X_{n,0}$ and $X_{n,1}$ at $t = 10.3$, at which the curve

† A copy of pages giving the technical details of these steps is available on request from either the authors or the JFM Editorial Office.
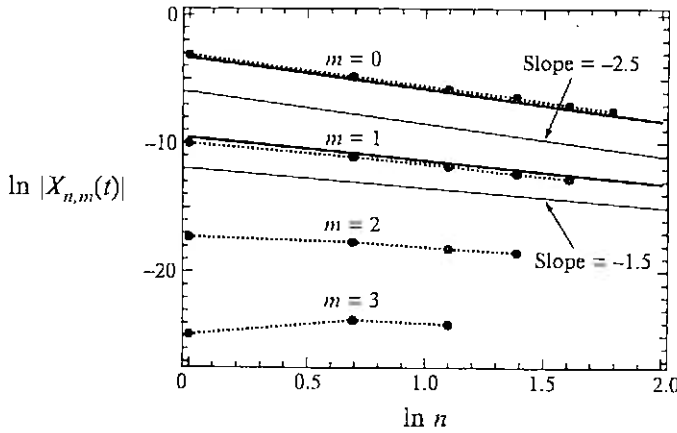
FIGURE 2. A plot of $\ln|X_{n,m}|$ vs. $\ln n$ at $t = 10.3$ by the numerical solution of the truncated set in the case $\epsilon_1 = \epsilon_2 = 0.001$ for $m = 0, 1, 2$ and 3 (dots with broken lines). Numerical values for $X_{n,0}$ and $X_{n,1}$ are compared with the asymptotic equations (6.3) (upper solid line) and (6.4) (lower solid line), respectively. The thin straight lines have the indicated slopes.

$\ln|X_{n,0}|$ vs. $\ln n$ fits best to a straight line. In the figure, $X_{n,2}$ and $X_{n,3}$ are also plotted. It can be observed that $X_{n,1}$ decays like $n^{-1.5}$, while $X_{n,0}$ decays like $n^{-2.5}$. This fact suggests that the sum

$$\sum_{n=-\infty}^{\infty} A_{n,\pm 1} \exp[i(n\lambda_1 \pm \lambda_2)] \tag{3.3}$$

loses analyticity at $t \approx 10.3$. Similar behaviour of $A_{n,0}$ and $A_{n,1}$ will be also obtained by asymptotic analysis in the next section.

4. The asymptotic behaviour of the Fourier coefficients

In this section we simplify the full system (2.21) by introducing the following ordering as in Moore (1979):

$$A_{n,m} = \epsilon_1^{|n|} \epsilon_2^{|m|} A_{n,m}^{(0)} + \epsilon_1^{|n|+2} \epsilon_2^{|m|} A_{n,m}^{(2,0)} + \cdots + \epsilon_1^{|n|} \epsilon_2^{|m|+2} A_{n,m}^{(0,2)} + \cdots. \tag{4.1}$$

Substituting this ordering into (2.21) yields an evolution equation for $A_{n,m}^{(i,j)}$. The number of terms in the resulting equation is finite, in contrast to (2.21). Retaining only the leading-order terms, we can obtain a closed set of equations for $\{A_{n,m}^{(0)}\}$ in the form

$$\frac{\mathrm{d}}{\mathrm{d}t} A_{n,m}^{(0)} = L A_{n,m}^{(0)} + P^{(0)}, \tag{4.2}$$

where $P^{(0)}$ may be written, in a symbolic notation, as

$$P^{(0)} \equiv \sum_{\{n,m\}}^{(2,0)} \{A^{(0)}\}^2 + \cdots + \sum_{\{n,m\}}^{(K,0)} \{A^{(0)}\}^K + \cdots + \sum_{\{n,m\}}^{(|n|+|m|,0)} \{A^{(0)}\}^{|n|+|m|}, \tag{4.3}$$

in which

$$\sum_{\{n,m\}}^{(K,0)} \equiv \begin{pmatrix} \text{sum with respect to} \quad n_1, \cdots, n_K, m_1, \cdots, m_K, \\ \text{satisfying} \\ n_1 + n_2 + \cdots + n_K = n, \ m_1 + m_2 + \cdots + m_K = m, \\ |n_1| + \cdots + |n_K| + |m_1| + \cdots + |m_K| = |n| + |m| \end{pmatrix}, \tag{4.4}$$

and $\{A^{(0)}\}^K$ stands for the terms of degree K in $A_{p,q}^{(0)}$. The reduced equation is linear in $A_{n,m}^{(0)}$ and the forcing term $P^{(0)}$ for $A_{n,\pm m}^{(0)}(n,m > 0)$ can be expressed in terms of $A_{p,q}^{(0)}$ where the p and q satisfy $0 \leqslant p \leqslant n$, $0 \leqslant \pm q \leqslant m$ and $0 < p \pm q < n + m$. In principle, the set of reduced equations can be solved recursively from small n and m. In practice, it is however not easy to solve the equations for n and m that are sufficiently large to derive the asymptotic behaviour of $A_{n,\pm m}^{(0)}$.

The results obtained in §3 suggest that the singularity develops at a time of $O(\ln \epsilon_1^{-1})$. It is therefore of interest to consider the simplification of the equations. For $|n| + |m| \leqslant 2$, (4.2) gives

$$\frac{\mathrm{d}}{\mathrm{d}t}X_{1,0}^{(0)} = \tfrac{1}{2}Z_{1,0}^{(0)}, \qquad \frac{\mathrm{d}}{\mathrm{d}t}X_{2,0}^{(0)} = \tfrac{1}{2}Z_{2,0}^{(0)} - \mathrm{i}X_{1,0}^{(0)}Z_{1,0}^{(0)},$$

$$\frac{\mathrm{d}}{\mathrm{d}t}Y_{1,0}^{(0)} = 0, \qquad \frac{\mathrm{d}}{\mathrm{d}t}Y_{2,0}^{(0)} = 0,$$

$$\frac{\mathrm{d}}{\mathrm{d}t}Z_{1,0}^{(0)} = \tfrac{1}{2}X_{1,0}^{(0)}, \qquad \frac{\mathrm{d}}{\mathrm{d}t}Z_{2,0}^{(0)} = \tfrac{1}{2}X_{2,0}^{(0)} + \tfrac{1}{2}(Z_{1,0}^{(0)2} - X_{1,0}^{(0)2}),$$

$$\frac{\mathrm{d}}{\mathrm{d}t}X_{0,1}^{(0)} = 0, \qquad \frac{\mathrm{d}}{\mathrm{d}t}X_{0,2}^{(0)} = 0,$$

$$\frac{\mathrm{d}}{\mathrm{d}t}Y_{0,1}^{(0)} = 0, \qquad \frac{\mathrm{d}}{\mathrm{d}t}Y_{0,2}^{(0)} = -\tfrac{1}{2}\mathrm{i}\delta^2 X_{0,1}^{(0)}Z_{0,1}^{(0)},$$

$$\frac{\mathrm{d}}{\mathrm{d}t}Z_{0,1}^{(0)} = \tfrac{1}{2}\delta X_{0,1}^{(0)}, \qquad \frac{\mathrm{d}}{\mathrm{d}t}Z_{0,2}^{(0)} = \tfrac{1}{2}\delta X_{0,2}^{(0)} - \tfrac{1}{2}\mathrm{i}\delta^2 X_{0,1}^{(0)}Y_{0,1}^{(0)},$$

$$\frac{\mathrm{d}}{\mathrm{d}t}X_{1,\pm 1}^{(0)} = \tfrac{1}{2}(1 + \delta^2)^{-1/2}Z_{1,\pm 1}^{(0)} + \tfrac{1}{2}\mathrm{i}\{1 - (1 + \delta^2)^{-1/2}\}X_{1,0}^{(0)}Z_{0,\pm 1}^{(0)},$$

$$\frac{\mathrm{d}}{\mathrm{d}t}Y_{1,\pm 1}^{(0)} = \pm\tfrac{1}{2}\delta(1 + \delta^2)^{-1/2}Z_{1,\pm 1}^{(0)} \mp \tfrac{1}{2}\mathrm{i}\delta(1 + \delta^2)^{-1/2}X_{1,0}^{(0)}Z_{0,\pm 1}^{(0)},$$

$$\frac{\mathrm{d}}{\mathrm{d}t}Z_{1,\pm 1}^{(0)} = \tfrac{1}{2}(1 + \delta^2)^{1/2}X_{1,\pm 1}^{(0)} - \tfrac{1}{2}\mathrm{i}\{1 - (1 + \delta^2)^{1/2}\}Z_{1,0}^{(0)}Z_{0,\pm 1}^{(0)}.$$

The solutions satisfying (2.14) and the above equations are given by

$$X_{1,0}^{(0)} = -\tfrac{1}{2}\mathrm{i}\sinh\tfrac{1}{2}t, \quad X_{2,0}^{(0)} = (\mathrm{i}/16)(t\sinh t - 2\cosh t + 2),$$

$$Y_{1,0}^{(0)} = 0, \qquad Y_{2,0}^{(0)} = 0,$$

$$Z_{1,0}^{(0)} = -\tfrac{1}{2}\mathrm{i}\cosh\tfrac{1}{2}t, \quad Z_{2,0}^{(0)} = (\mathrm{i}/16)(t\cosh t - 3\sinh t),$$

$$X_{0,1}^{(0)} = -\tfrac{1}{2}\mathrm{i}, \qquad X_{0,2}^{(0)} = 0,$$

$$Y_{0,1}^{(0)} = 0, \qquad Y_{0,2}^{(0)} = (\mathrm{i}/32)\delta^3 t^2,$$

$$Z_{0,1}^{(0)} = -\tfrac{1}{4}\mathrm{i}\delta t, \quad Z_{0,2}^{(0)} = 0,$$

$$X_{1,\pm 1}^{(0)} = \mp(\mathrm{i}/32)\delta Ct^2 \sinh\tfrac{1}{2}t,$$

$$Y_{1,\pm 1}^{(0)} = (\mathrm{i}/32)\delta^2(1 + \delta^2)^{-1/2}\{(-Ct^2 + 4t - 8C)\cosh\tfrac{1}{2}t + (4Ct - 8)\sinh\tfrac{1}{2}t + 8C\},$$

$$Z_{1,\pm 1}^{(0)} = \mp(\mathrm{i}/32)\delta(1 + \delta^2)^{1/2}Ct^2 \cosh\tfrac{1}{2}t,$$

where

$$C \equiv 1 - (1 + \delta^2)^{-1/2},$$

so that

$$X_{1,0}^{(0)} = i\left(-\tfrac{1}{4}\right)\{e^{t/2} + O(e^{-t/2})\}, \quad X_{2,0}^{(0)} = i\left(-\tfrac{1}{4}\right)^2\{\left(\tfrac{1}{2}t - 2\right)e^t + O(1)\},$$

$$Y_{1,0}^{(0)} = 0, \qquad\qquad\qquad\qquad Y_{2,0}^{(0)} = 0,$$

$$Z_{1,0}^{(0)} = i\left(-\tfrac{1}{4}\right)\{e^{t/2} + O(e^{-t/2})\}, \quad Z_{2,0}^{(0)} = i\left(-\tfrac{1}{4}\right)^2\{\left(\tfrac{1}{2}t - \tfrac{3}{2}\right)e^t + O(1)\},$$

and

$$X_{1,\pm 1}^{(0)} = i\left(\mp\tfrac{1}{4}\delta\right)\left(-\tfrac{1}{4}\right)e^{t/2}\left\{-[1 - (1 + \delta^2)^{-1/2}]t^2 + O(t)\right\} + O(1),$$

$$Y_{1,\pm 1}^{(0)} = i\left(\mp\tfrac{1}{4}\delta\right)\left(-\tfrac{1}{4}\right)e^{t/2}\left\{\mp\delta[1 - (1 + \delta^2)^{-1/2}]t^2 + O(t)\right\} + O(1),$$

$$Z_{1,\pm 1}^{(0)} = i\left(\mp\tfrac{1}{4}\delta\right)\left(-\tfrac{1}{4}\right)e^{t/2}\left\{-[(1 + \delta^2)^{1/2} - 1]t^2 + O(t)\right\} + O(1),$$

for large t. These suggest that $A_{n,m}^{(0)}$ behaves like $e^{|n|t/2}t^{|n|-1+2|m|}$ for large t, and $A_{n,\pm m}^{(0)}$ may be expressed as

$$A_{n,\pm m}^{(0)} = i\left(\mp\frac{\delta}{4}\right)^m\left(-\frac{1}{4}\right)^n e^{nt/2}\left[a_{n,\pm m}^{(0)}t^{n-1+2m} + a_{n,\pm m}^{(1)}t^{n-2+2m} + \cdots\right] + O(e^{(n-1)t/2}), \quad (4.5)$$

for $n > 0$ and $m \geqslant 0$. It can be shown inductively that this time dependence is consistent with (4.2) under the initial condition (2.14). Estimation of $P^{(0)}$ in (4.2) shows that $\{A^{(0)}\}^K$ is of order $e^{nt/2}t^{n-K+2m}$. Because $e^{nt/2}$ is a solution of the homogeneous part of the equation for $A_{n,\pm m}^{(0)}$, the term $\{A^{(0)}\}^K$ yields a contribution of order $e^{nt/2}t^{n-K+2m+1}$ to the solution. Thus the terms quadratic in $P^{(0)}$ yields the dominant contributions of order $e^{nt/2}t^{n+2m-1}$ to $A_{n,\pm m}^{(0)}$ at large t.

Note that (4.1) and (4.5) give

$$X_{n,\pm(m+1)}/X_{n,\pm m} = O(\epsilon_2 t^2), \tag{4.6}$$

for large t and small $\epsilon = \max(\epsilon_1, \epsilon_2)$, and similar expressions for Y and Z. Since the time t under consideration is $O(\ln\epsilon_1^{-1})$, (4.6) implies that when ϵ_2 is small enough, the Fourier coefficients for small m are important. In the following, we therefore consider the behaviour of $A_{n,0}^{(0)}$ and $A_{n,\pm 1}^{(0)}$ at large t.

Since $A_{n,0}^{(0)}$ does not interact with spanwise modes at order $O(\epsilon_1^{|n|})$, the equation for $A_{n,0}^{(0)}$ can be reduced to (1.4) that is derived from the two-dimensional vortex sheet equation (the Birkhoff–Rott equation). Hence, it is clear that the analysis of $A_{n,0}^{(0)}$ would yield the same results as in Moore (1979). However, in order to proceed to the analysis of $A_{n,\pm 1}^{(0)}$, it is convenient to analyse $A_{n,0}^{(0)}$ on the basis of (4.2) rather than (1.4). We therefore briefly review here the analysis based on (4.2) before proceeding to the analysis of $A_{n,\pm 1}^{(0)}$.

Retaining only the terms that yield the leading-order contribution for large t to the solution gives for $n \geqslant 1$,

$$\frac{\mathrm{d}}{\mathrm{d}t}X_{n,0}^{(0)} = \tfrac{1}{2}nZ_{n,0}^{(0)} + \sum_{k=1}^{n-1} -ik(n-k)X_{k,0}^{(0)}Z_{n-k,0}^{(0)}, \tag{4.7a}$$

$$\frac{\mathrm{d}}{\mathrm{d}t} Y_{n,0}^{(0)} = 0, \tag{4.7b}$$

$$\frac{\mathrm{d}}{\mathrm{d}t} Z_{n,0}^{(0)} = \tfrac{1}{2} n X_{n,0}^{(0)} + \sum_{k=1}^{n-1} \tfrac{1}{2} ik(n-k)(Z_{k,0}^{(0)} Z_{n-k,0}^{(0)} - X_{k,0}^{(0)} X_{n-k,0}^{(0)}), \tag{4.7c}$$

where the sum $\sum_{k=1}^{n}$ is zero when $n < 1$. Note that the right-hand side of the equation does not include $Y^{(0)}$. Substitution of (4.5) into (4.7a–c) gives recursive relations for $a_{n,0}^{(0)} \equiv (a_{n,0}^{(0)}, b_{n,0}^{(0)}, c_{n,0}^{(0)})$ as

$$a_{1,0}^{(0)} = c_{1,0}^{(0)} = 1, \quad b_{1,0}^{(0)} = 0, \tag{4.8}$$

and, for $n \geqslant 2$,

$$a_{n,0}^{(0)} = c_{n,0}^{(0)} = \frac{1}{2(n-1)} \sum_{k=1}^{n-1} k(n-k) c_{k,0}^{(0)} c_{n-k,0}^{(0)}, \quad b_{n,0}^{(0)} = 0. \tag{4.9}$$

The relations (4.8) and (4.9) are equivalent to (3.4) and (3.5) in Moore (1979), and we have for large n and t,

$$\left. \begin{array}{c} X_{n,0}^{(0)} \\ Z_{n,0}^{(0)} \end{array} \right\} \sim i \left(-\tfrac{1}{4} \right)^n e^{nt/2} \left[(2\pi)^{-1/2} e^n n^{-5/2} t^{n-1} + a_{n,0}^{(1)} t^{n-2} + \cdots \right], \tag{4.10}$$

The leading term may be rearranged to give

$$\left. \begin{array}{c} \epsilon_1^n X_{n,0}^{(0)} \\ \epsilon_1^n Z_{n,0}^{(0)} \end{array} \right\} \sim (2\pi)^{-1/2} (-1)^n t^{-1} n^{-5/2} \exp[n(1 + \tfrac{1}{2} t + \ln \tfrac{1}{4} \epsilon_1 t)]. \tag{4.11}$$

Note that (4.11) is valid only for $n \gg 1$ and $t \gg 1$ and $n \ll t$ (see Moore 1979). Thus the exponential decay with respect to n of the coefficients fails at a time t_c defined by $1 + \tfrac{1}{2} t + \ln \tfrac{1}{4} \epsilon_1 t = 0$. The singularity associated with $A_{n,0}$ can be obtained by the following approximate summation of the Fourier coefficients:

$$\left. \begin{array}{c} x - \lambda_1 \\ z \end{array} \right\} = \frac{2\sqrt{2}}{3} it_c^{-1} \{ [1 - e^{i(\lambda_1 - \pi)}]^{3/2} - [1 - e^{-i(\lambda_1 - \pi)}]^{3/2} \} + \varphi, \tag{4.12}$$

where φ stands for less singular terms (and where a typographical error in Moore (1979) has been corrected). The singularity appears at $\lambda_1 = (2k+1)\pi$ with k being an integer. Let $\Lambda_1 \equiv \lambda_1 - (2k+1)\pi$. Then for small $|\Lambda_1|$, (4.12) gives

$$\left. \begin{array}{c} x - \lambda_1 \\ z \end{array} \right\} \approx (\mathrm{sgn} \Lambda_1) \tfrac{4}{3} t_c^{-1} |\Lambda_1|^{3/2} + \varphi.$$

Now let us proceed to the analysis of $a_{n,\pm 1}^{(0)} \equiv (a_{n,\pm 1}^{(0)}, b_{n,\pm 1}^{(0)}, c_{n,\pm 1}^{(0)})$. In the same way as for $a_{n,0}^{(0)}$, we have for $n \geqslant 0$,

$$\frac{\mathrm{d}}{\mathrm{d}t} X_{n,\pm 1}^{(0)} = \frac{1}{2} \frac{n^2}{(n^2 + \delta^2)^{1/2}} Z_{n,\pm 1}^{(0)}$$

$$+ \sum_{k=1}^{n-1} \frac{i}{2} \left\{ (n-k)[(n-k)^2 + \delta^2]^{1/2} + k|k| - n(n^2 + \delta^2)^{1/2} \right\} X_{n-k,\pm 1}^{(0)} Z_{k,0}^{(0)}$$

$$+ \sum_{k=1}^{n} \frac{i}{2} \left\{ \frac{(n-k)^3}{[(n-k)^2 + \delta^2]^{1/2}} + k|k| - \frac{n^3}{(n^2 + \delta^2)^{1/2}} \right\} X_{k,0}^{(0)} Z_{n-k,\pm 1}^{(0)}, \tag{4.13a}$$

$$\frac{\mathrm{d}}{\mathrm{d}t} Y_{n,\pm 1}^{(0)} = \frac{1}{2} \frac{\pm n\delta}{(n^2 + \delta^2)^{1/2}} Z_{n,\pm 1}^{(0)}, \tag{4.13b}$$

$$\frac{\mathrm{d}}{\mathrm{d}t} Z_{n,\pm 1}^{(0)} = \frac{1}{2}(n^2 + \delta^2)^{1/2} X_{n,\pm 1}^{(0)}$$

$$+ \sum_{k=1}^{n-1} \frac{i}{2} \left\{ (n-k)[(n-k)^2 + \delta^2]^{1/2} + k|k| - n(n^2 + \delta^2)^{1/2} \right\} X_{n-k,\pm 1}^{(0)} X_{k,0}^{(0)}$$

$$- \sum_{k=1}^{n} \frac{i}{2} \left\{ (n-k)[(n-k)^2 + \delta^2]^{1/2} + k|k| - n(n^2 + \delta^2)^{1/2} \right\} Z_{k,0}^{(0)} Z_{n-k,\pm 1}^{(0)}. \tag{4.13c}$$

Substituting (4.5) into (4.13a–c) yields the relations for $n \geqslant 1$,

$$2n(n+1)c_{n,\pm 1}^{(0)} = \sum_{k=1}^{n} \left\{ n^2 k - (n^2 - nk + k^2)(n^2 + \delta^2)^{1/2} + \frac{k(n-k)^2(n^2 + \delta^2)^{1/2}}{[(n-k)^2 + \delta^2]^{1/2}} \right.$$

$$\left. + \frac{n(n-k)(n^2 - nk + \delta^2)}{[(n-k)^2 + \delta^2]^{1/2}} \right\} c_{n-k,\pm 1}^{(0)} a_{k,0}^{(0)}, \tag{4.14a}$$

$$a_{n,\pm 1}^{(0)} = \frac{n}{(n^2 + \delta^2)^{1/2}} c_{n,\pm 1}^{(0)}, \tag{4.14b}$$

$$b_{n,\pm 1}^{(0)} = \frac{\pm \delta}{(n^2 + \delta^2)^{1/2}} c_{n,\pm 1}^{(0)}. \tag{4.14c}$$

Since $a_{n,0}^{(0)}$ are known, $a_{n,\pm 1}^{(0)}$, $b_{n,\pm 1}^{(0)}$ and $c_{n,\pm 1}^{(0)}$ for $n \geqslant 1$ can be obtained from (4.14a–c) with $a_{0,\pm 1}^{(0)} = b_{0,\pm 1}^{(0)} = 0$ and $c_{0,\pm 1}^{(0)} = 1$, which is a consequence of the solution of the equation for $A_{0,\pm 1}^{(0)}$. It is readily seen that all of $(a_{n,\pm 1}^{(0)}, b_{n,\pm 1}^{(0)}, c_{n,\pm 1}^{(0)})$ are real numbers. The numerical solutions of (4.14a) are plotted for some aspect ratios $\delta = 0.1, 1, 10$ in figure 3. It can be observed in the figure that $c_{n,\pm 1}^{(0)}$ behaves like $e^n n^{-3/2}$ for large n independently of δ, while $c_{n,0}^{(0)}$ behaves like $e^n n^{-5/2}$. It is seen from (4.14b) and (4.14c) that $a_{n,\pm 1}^{(0)}$ and $b_{n,\pm 1}^{(0)}$ then behave like $e^n n^{-3/2}$ and $e^n n^{-5/2}$, respectively, for large $n(\gg \delta)$. From these results and (4.5), we have for large t and $n(\gg \delta)$,

$$\epsilon_1^n \epsilon_2 \begin{pmatrix} X_{n,\pm 1}^{(0)} \\ Y_{n,\pm 1}^{(0)} \\ Z_{n,\pm 1}^{(0)} \end{pmatrix} \sim \mp \frac{i}{4} (-1)^n \delta \epsilon_2 C_\delta \begin{pmatrix} n^{-3/2} \\ \pm \delta n^{-5/2} \\ n^{-3/2} \end{pmatrix} f(t), \tag{4.15}$$

where

$$f(t) \equiv t \exp[n(1 + \tfrac{1}{2}t + \ln \tfrac{1}{4}\epsilon_1 t)],$$

and C_δ is a constant depending only on the aspect ratio δ. The above results are consistent with those obtained in §3.

When δ is small, C_δ can be estimated as shown below. (Note that small value of δ corresponds to large wavelength of the initial disturbance in the spanwise direction.) Putting $n = 1$ in (4.14a) gives

$$4c_{1,\pm 1}^{(0)} = \left[1 - (1 + \delta^2)^{1/2} \right] a_{1,0}^{(0)} c_{0,\pm 1}^{(0)} \approx -\tfrac{1}{2}\delta^2, \tag{4.16}$$
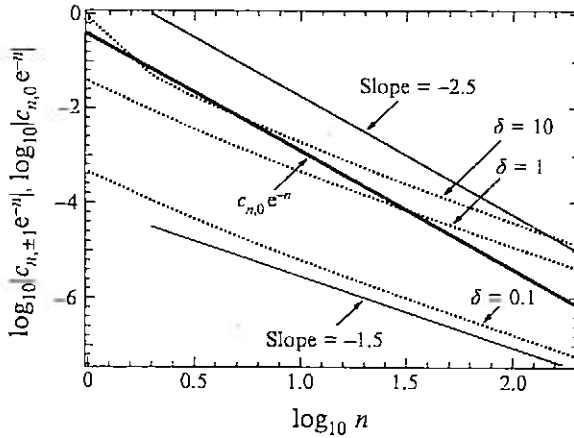
FIGURE 3. A plot of $\log_{10}|c_{n,\pm1}e^{-n}|$ *vs.* $\log_{10}n$ by the numerical solutions of (4.14a) for the aspect ratio $\delta = 0.1, 1$ and 10 (broken lines). The values of $\log_{10}|c_{n,0}e^{-n}|$ are also plotted(solid line). The thin straight lines have the indicated slopes.

where $a_{1,0}^{(0)} = c_{0,\pm1}^{(0)} = 1$. Since $a_{k,0}^{(0)} = O(\delta^0)$ for $k \geqslant 1$, (4.14a) and (4.16) imply that $c_{n,\pm1}^{(0)}$ are $O(\delta^2)$ for $n \geqslant 1$. By retaining terms of $O(\delta^2)$ in (4.14a), we have, for $n \geqslant 2$,

$$(n+1)c_{n,\pm1}^{(0)} = \sum_{k=1}^{n-1} k(n-k)c_{n-k,\pm1}^{(0)}a_{k,0}^{(0)}. \tag{4.17}$$

Let $g(x)$ and $h(x)$ be functions defined by

$$g(x) \equiv a_{1,0}^{(0)}x + a_{2,0}^{(0)}x^2 + a_{3,0}^{(0)}x^3 + \cdots, \tag{4.18a}$$

$$h(x) \equiv c_{1,\pm1}^{(0)}x + c_{2,\pm1}^{(0)}x^2 + c_{3,\pm1}^{(0)}x^3 + \cdots. \tag{4.18b}$$

Then (4.17) is equivalent to

$$\frac{\mathrm{d}}{\mathrm{d}x}[xh(x)] = x^2\left[\frac{\mathrm{d}}{\mathrm{d}x}g(x)\right]\left[\frac{\mathrm{d}}{\mathrm{d}x}h(x)\right] + 2c_{1,\pm1}^{(0)}x. \tag{4.19}$$

The function $g(x)$ is the same one as used in Moore (1979), and may be written as

$$g(x) = u(x) - \tfrac{1}{2}u^2(x), \quad x = ue^{-u}.$$

Since $u(x)$ is a two-valued function with a singularity at $x = e^{-1}$, $g(x)$ is also singular at $x = e^{-1}$ and can be expanded near the singularity as

$$g(x) = \tfrac{1}{2} - y + \tfrac{2}{3}\sqrt{2}y^{3/2} - \tfrac{5}{6}y^2 + O(y^{5/2}),$$

where $y = 1 - ex$. Note that $a_{n,0}^{(0)} \sim (2\pi)^{-1/2}e^n n^{-5/2}$ in (4.10) is determined from the dominant singular term $(2\sqrt{2}/3)(1 - ex)^{3/2}$ in $g(x)$.

Equation (4.19) can be rewritten in terms of u as

$$\frac{\mathrm{d}}{\mathrm{d}u}(uh) = 2c_{1,\pm1}^{(0)}ue^{-u},$$

and integrated to give

$$h(x) = 2c_{1,\pm1}^{(0)}\frac{1 - [u(x) + 1]e^{-u(x)}}{u(x)}.$$

The function $h(x)$ is also singular at $x = e^{-1}$ and can be expanded as

$$h(x) = 2c_{1,\pm1}^{(0)} \left[\left(1 - \frac{2}{e}\right) + \sqrt{2}\left(1 - \frac{3}{e}\right)y^{1/2} + \frac{4}{3}\left(1 - \frac{3}{e}\right)y + O(y^{3/2}) \right],$$

near $y = 0$. The dominant singular behaviour of h is given by $2c_{1,\pm1}^{(0)}\sqrt{2}(1 - 3/e) \times (1 - ex)^{1/2}$. Hence $c_{n,\pm1}^{(0)}$ behaves like

$$c_{n,\pm1}^{(0)} \sim c_{1,\pm1}^{(0)} \left(\frac{2}{\pi}\right)^{1/2} \left(\frac{3}{e} - 1\right) e^n n^{-3/2} \quad \text{as} \quad n \to \infty, \tag{4.20}$$

where we have used the binomial theorem. The approximation leading to (4.20) is only valid if $\delta \ll 1$; then, from (4.5), (4.16) and (4.20), we have for large n and t,

$$\epsilon_2 \epsilon_1^n Z_{n,\pm1}^{(0)} \approx i\left(\mp\frac{\delta\epsilon_2}{4}\right)\left(\frac{2}{\pi}\right)^{1/2}\left(\frac{3}{e} - 1\right)\left(-\frac{\delta^2}{8}\right)(-1)^n n^{-3/2} f(t). \tag{4.21}$$

Making the comparison between (4.15) and (4.21), we have

$$C_\delta \approx \left(\frac{2}{\pi}\right)^{1/2}\left(\frac{3}{e} - 1\right)\left(-\frac{\delta^2}{8}\right), \tag{4.22}$$

provided that δ is small.

5. The evolution of spanwise disturbance

All of the eigenvalues of the linear matrix L in (2.22) are zero when $n = 0$. The mode $A_{0,m}^{(0)}$ does not therefore grow exponentially in t, in contrast to $A_{n,0}^{(0)}$ and $A_{n,\pm1}^{(0)}$. Integration of $A_{0,m}^{(0)}$ for some small m suggests that if the initial condition is given by

$$X_{0,\pm1}^{(0)}(0) = 0, \;\; Y_{0,1}^{(0)}(0) = Y_{0,-1}^{(0)}(0)^* \neq 0, \;\; Z_{0,1}^{(0)}(0) = Z_{0,-1}^{(0)}(0)^* \neq 0,$$

$$A_{0,\pm m}^{(0)}(0) = (0,0,0), \quad \text{for } m > 1,$$

where an asterisk denotes complex conjugate, then $A_{0,m}^{(0)}$ for $m \geqslant 2$ remains zero for $t > 0$. This suggests that $A_{0,m}^{(0)}$ can grow only if $X_{0,\pm1}^{(0)}(0) \neq 0$. The initial disturbance (2.14) corresponds to this case. This is another reason why we chose (2.14). Taking account of this fact, we shall consider in the following the evolution of a spanwise disturbance subject to the initial condition $(X_{0,1}^{(0)}(0) = -X_{0,-1}^{(0)}(0) = -\frac{1}{2}i)$.

We have seen in §4 that since $A_{n,0}^{(0)}$ does not interact with spanwise modes at $O(\epsilon_1^{|n|})$, the analysis of $A_{n,0}^{(0)}$ is equivalent to that of $A_n^{(0)}$ whose equation is derived from the two-dimensional vortex sheet equation. Similarly since $A_{0,m}^{(0)}$ does not interact with streamwise modes at $O(\epsilon_2^{|m|})$, the analysis of $A_{0,m}^{(0)}$ can be made through a reduced equation which has only one independent variable (except time) such as the Birkhoff–Rott equation. Here we derive the reduced equation which describes the evolution of a spanwise disturbance and determines the asymptotic behaviour of the spanwise mode.

Let the vortex sheet be expressed in the form

$$R(\lambda_1, \lambda_2, t) = (\lambda_1 + x(\lambda_2, t), y(\lambda_2, t), z(\lambda_2, t)), \tag{5.1}$$

and $\gamma(\lambda_1)$ in (2.4) be constant, say γ_0, then $W \equiv \gamma_0 \partial R/\partial\lambda_2$ does not depend on λ_1. By

putting $\lambda'_1 = \lambda_1 + \alpha$, $x = x(\lambda_2, t)$, $x' = x(\lambda'_2, t)$ and so on, and

$$X = R(\lambda_1, \lambda_2, t) - R(\lambda'_1, \lambda'_2, t) = (-\alpha + x - x', \ y - y', \ z - z'),$$

and noting

$$\int_{-\infty}^{\infty} \frac{-\alpha + A}{\{(-\alpha + A)^2 + B^2\}^{3/2}} \, d\alpha = 0, \quad \int_{-\infty}^{\infty} \frac{1}{\{(-\alpha + A)^2 + B^2\}^{3/2}} \, d\alpha = \frac{2}{B^2},$$

for any constants A and $B \neq 0$, we may rewrite (2.11) as

$$\frac{\partial}{\partial t} \begin{pmatrix} x(\lambda_2, t) \\ y(\lambda_2, t) \\ z(\lambda_2, t) \end{pmatrix} = -\frac{1}{2\pi} \text{p.v.} \int_{-\infty}^{\infty} \frac{d\lambda'_2}{(y - y')^2 + (z - z')^2} \begin{pmatrix} 0 \\ y - y' \\ z - z' \end{pmatrix} \times \frac{\partial}{\partial \lambda'_2} \begin{pmatrix} x' \\ y' \\ z' \end{pmatrix}. \quad (5.2)$$

In terms of $\zeta = \zeta(\lambda_2, t) \equiv y + iz$, this may be also written as

$$\frac{\partial}{\partial t} x(\lambda_2, t) = -\frac{1}{2\pi} \text{p.v.} \int_{-\infty}^{\infty} \frac{(y - y')\dfrac{\partial}{\partial \lambda'_2} z' - (z - z')\dfrac{\partial}{\partial \lambda'_2} y'}{(y - y')^2 + (z - z')^2} \, d\lambda'_2$$

$$= \text{Im} \left\{ -\frac{1}{2\pi} \text{p.v.} \int_{-\infty}^{\infty} \frac{\dfrac{\partial}{\partial \lambda'_2}(\zeta - \zeta')^{\bullet}}{(\zeta - \zeta')^{\bullet}} \, d\lambda'_2 \right\}$$

$$= \frac{1}{2\pi} \text{Im} \left\{ \text{p.v.} \int_{-\infty}^{\infty} \frac{\partial}{\partial \lambda'_2} \ln(\zeta - \zeta') \, d\lambda'_2 \right\}, \quad (5.3)$$

and

$$\frac{\partial}{\partial t} \zeta(\lambda_2, t)^{\bullet} = \frac{1}{2\pi i} \text{p.v.} \int_{-\infty}^{\infty} \frac{\dfrac{\partial}{\partial \lambda'_2} x'}{\zeta - \zeta'} \, d\lambda'_2, \quad (5.4)$$

where $\zeta' = \zeta(\lambda'_2, t)$. Let θ and β be defined by $\eta(\beta, t) \equiv \zeta(\lambda_2, t) - \zeta(\lambda_2 + \beta, t) \equiv re^{i\theta}$. Then it is readily seen that the integral in (5.3) can be reduce to an integral of θ with respect to β, and is equal to zero when $\text{Arg}[\eta(\beta, t)/\eta(-\beta, t)] \to \pi$ as $\beta \to \infty$. The vortex sheet whose initial shape is given by

$$R(\lambda_1, \lambda_2, 0) = (\lambda_1 + \epsilon_2 \sin \delta \lambda_2, \ \lambda_2, \ 0) \quad (5.5)$$

keeps the integral in (5.3) at zero and does not change position in the streamwise (x) direction. In the spanwise (y) direction, the sheet is $2\pi/\delta$-periodic in λ_2 ($b\gamma_0/U$-periodic in physical space), and it can therefore be expanded in the Fourier series such as

$$\zeta(\lambda_2, t) = \lambda_2 + \sum_{m=-\infty}^{\infty} A[m](t) e^{i\delta m \lambda_2}. \quad (5.6)$$

Substituting (5.6) and $\lambda'_2 = \lambda_2 + \beta$ into (5.4) gives

$$\sum_{m=-\infty}^{\infty} \frac{d}{dt} A[-m]^{\bullet}(t) e^{i\delta m \lambda_2} = -\frac{\epsilon_2}{2\pi i} \text{p.v.} \int_{-\infty}^{\infty} \frac{d\beta}{\beta} \left\{ \tfrac{1}{2}\delta e^{i\delta(\lambda_2 + \beta)} + \tfrac{1}{2}\delta e^{-i\delta(\lambda_2 + \beta)} \right\}$$

$$\times \left\{ 1 + \frac{s}{\beta} + \frac{s^2}{\beta^2} + \cdots \right\}, \quad (5.7)$$

where

$$s = \sum_{m=-\infty}^{\infty} A[m](t)e^{i\delta m \lambda_2}(1 - e^{i\delta m \beta}).$$

In order to simplify the notation, we put $\hat{t} \equiv \delta t$, $\hat{A}[m](\hat{t}) \equiv \delta A[m](t)$ and $\hat{\epsilon}_2 \equiv \delta \epsilon_2$, and we shall hereafter omit the hats up to (5.18). Equating coefficients of $e^{i\delta m \lambda_2}$ gives the following equation for $A[m](t)$:

$$
\begin{aligned}
\frac{dA[-m]^*}{dt} = -\frac{\epsilon_2}{4\pi i} \Big\{ & A[m-1]J(m) + A[m+1]K(m) + \cdots \\
& + \sum_{m_1+m_2+\cdots+m_k=m-1} A[m_1]A[m_2]\cdots A[m_k]J(m_1, m_2, \cdots, m_k) \\
& + \sum_{m_1+m_2+\cdots+m_k=m+1} A[m_1]A[m_2]\cdots A[m_k]K(m_1, m_2, \cdots, m_k) \\
& + \cdots \Big\},
\end{aligned}
\tag{5.8}
$$

where

$$J(m_1, \cdots, m_k) = \text{p.v.} \int_{-\infty}^{\infty} e^{i\beta}(1 - e^{im_1\beta})\cdots(1 - e^{im_k\beta})\beta^{-(k+1)}d\beta,$$

$$K(m_1, \cdots, m_k) = \text{p.v.} \int_{-\infty}^{\infty} e^{-i\beta}(1 - e^{im_1\beta})\cdots(1 - e^{im_k\beta})\beta^{-(k+1)}d\beta.$$

It may be interesting to note that (5.8) is the same as (2.2) in Meiron *et al.* (1982) except that the dominant I-term in their equation is absent from (5.8). By introducing the ordering $A[m] = O(\epsilon_2^{|m|})$ and its associated expansion

$$A[m] = \epsilon_2^{|m|}A^{(0)}[m] + \epsilon_2^{|m|+2}A^{(2)}[m] + \cdots, \tag{5.9}$$

we divide (5.8) into subsystems for $A^{(0)}[m]$, $A^{(2)}[m]$, $\cdots$, as in §4. Regarding the subsystem for $A^{(0)}[m](m > 0)$, only the sums involving the integral $J(m_1, m_2, \cdots, m_k)$ for $m_1, m_2, \cdots, m_k > 0$ contribute to the leading order. Since all the arguments of J are positive it can be evaluated by residues:

$$J(m_1, m_2, \cdots, m_k) = \pi i(-i)^k m_1 m_2 \cdots m_k.$$

Thus we have

$$\frac{d}{dt}A^{(0)}[1]^* = \tfrac{1}{4}, \tag{5.10a}$$

$$
\begin{aligned}
\frac{d}{dt}A^{(0)}[m]^* = \tfrac{1}{4}\Big\{ & (-i)(m-1)A^{(0)}[m-1] + \cdots \\
& + \sum_{m_1+\cdots+m_k=m-1} (-i)^k m_1 \cdots m_k A^{(0)}[m_1] \cdots A^{(0)}[m_k] + \cdots \\
& + (-i)^{m-1}(A^{(0)}[1])^{m-1}\Big\},
\end{aligned}
\tag{5.10b}
$$

where $m > 1$ and we have used $A[-m] = -A[m]$. Note that (5.10b) is also obtained by taking the limit $1/\delta \to 0$ in (4.2).

The solution for (5.10a,b) can be written as

$$A^{(0)}[m] = \left(\tfrac{1}{4}t\right)^m \{a^{(0)}[m] + a^{(1)}[m]t^{-1} + \cdots + a^{(m)}[m]t^{-m}\}. \tag{5.11}$$

Substitution of (5.11) into (5.10a,b) gives

$$a^{(0)}[1] = 1, \tag{5.12a}$$

$$ma^{(0)}[m]^{\bullet} = (-i)(m-1)a^{(0)}[m-1] + \cdots$$
$$+ \sum_{m_1 + \cdots + m_k = m-1} (-i)^k m_1 \cdots m_k a^{(0)}[m_1] \cdots a^{(0)}[m_k] + \cdots$$
$$+ (-i)^{m-1}(a^{(0)}[1])^{m-1}. \tag{5.12b}$$

Let $q(x)$ be a complex-valued generating function of real variable x defined by

$$q(x) \equiv a^{(0)}[1]x + a^{(0)}[2]x^2 + \cdots . \tag{5.13}$$

Then (5.12a,b) are equivalent to

$$q'(0) = 1, \tag{5.14}$$

$$q'(x)^{\bullet} - 1 = -ixq'(x)\{1 + (-ixq'(x)) + (-ixq'(x))^2 + \cdots\}$$
$$= \frac{-ixq'(x)}{1 + ixq'(x)}, \tag{5.15}$$

where a prime denotes the differentiation with respect to x and we have assumed that $|ixq'(x)| < 1$. Equation (5.15) is rearranged to give

$$q'(x)^{\bullet} - 1 = -ixq'(x)q'(x)^{\bullet}.$$

Since the right-hand side of the above equation is pure imaginary, we have

$$p(x) = x(1 + p(x)^2),$$

where $ip(x) \equiv q'(x) - 1$. The solution which satisfies condition (5.14), i.e. $p(0) = 0$, is

$$p(x) = \frac{1 - (1 - 4x^2)^{1/2}}{2x},$$

and its integration with respect to x gives

$$q(x) = x + \frac{i}{2}\left\{1 - (1 - 4x^2)^{1/2} + \ln\frac{1 + (1 - 4x^2)^{1/2}}{2}\right\}, \tag{5.16}$$

in which the integration constant has been determined to satisfy $q(0) = 0$. $q(x)$ has a singularity at $x = \frac{1}{2}$ and the dominant singular behaviour of q is given by $(i/6)(1 - 4x^2)^{3/2}$. It follows that $a^{(0)}[m]$ behaves as

$$a^{(0)}[2k] \sim i\frac{1}{8\sqrt{\pi}}k^{-5/2}4^k, \quad a^{(0)}[2k-1] \sim 0 \quad \text{as} \quad k \to \infty. \tag{5.17}$$

Taking into account (5.9) and (5.11), we have for large k and t

$$\epsilon_2^{2k}A^{(0)}[2k] \sim i\frac{1}{8\sqrt{\pi}}k^{-5/2}\left(\frac{\epsilon_2 t}{2}\right)^{2k}, \quad \epsilon_2^{2k-1}A^{(0)}[2k-1] \sim 0. \tag{5.18}$$

Equation (5.18) implies that a singularity appears in the spanwise (y) direction at

$$\hat{t}_c^{(\text{span})} = \frac{2}{\hat{\epsilon}_2}, \tag{5.19}$$

and, at that instant, the Fourier coefficient $\hat{A}[m]$ is $O(1)$ and behaves like $m^{-5/2}$. From (5.6), (5.9) and (5.18), we have, at $\hat{t} = \hat{t}_c^{(\mathrm{span})}$,

$$\zeta - \lambda_2 = (\mathrm{i}/6)\{(1 - \mathrm{e}^{2\mathrm{i}\delta\lambda_2})^{3/2} - (1 - \mathrm{e}^{-2\mathrm{i}\delta\lambda_2})^{3/2}\} + \varphi, \tag{5.20}$$

where φ stands for less singular terms. The singularity appears at $\lambda_2 = k\pi/\delta$ where k is an integer. For small $|\Lambda_2|$, where $\Lambda_2 \equiv \lambda_2 - k\pi/\delta$, (5.20) gives

$$\zeta - \Lambda_2 \approx (\mathrm{sgn}\Lambda_2)\tfrac{2}{3}|\delta\Lambda_2|^{3/2} + \varphi. $$

Note that only the y-component is singular at $\Lambda_2 = 0$.

6. Discussion and conclusions

In this paper, we have considered the three-dimensional evolution of a periodic perturbation in both the streamwise and spanwise directions applied initially to a flat and uniform vortex sheet. In order to make the problem analytically tractable, we have assumed the amplitude of disturbance to be small but finite. The double periodic shape of the sheet at $t > 0$ is expressed in a Fourier series as a function of two Lagrangian parameters. The evolution equations for the Fourier coefficients $A_{n,m}(t) \equiv (X_{n,m}, Y_{n,m}, Z_{n,m})$ are derived on the basis of a Lagrangian representation of the motion of the vortex sheet. The subscripts n and m of $A_{n,m}(t)$ denote the wavenumbers in the streamwise and spanwise directions, respectively.

The asymptotic analyses of §4 for the behaviour of the Fourier coefficients at large t show that $A_{n,0}$ and $A_{n,\pm 1}$ behave like

$$X_{n,0}, Z_{n,0} = O(t_c^{-1}) \text{ and } X_{n,\pm 1}, Y_{n,\pm 1}, Z_{n,\pm 1} = O(\epsilon_2 t_c) \text{ for } n > 0 \tag{6.1}$$

and

$$X_{n,0}, Z_{n,0}, Y_{n,\pm 1} \propto n^{-5/2} \text{ and } X_{n,\pm 1}, Z_{n,\pm 1} \propto n^{-3/2} \text{ for large } n, \tag{6.2}$$

at a time $t_c (= O(\ln(\epsilon_1^{-1})) \gg 1)$ defined by $1 + \tfrac{1}{2}t_c + \ln\tfrac{1}{4}\epsilon_1 t_c = 0$, where ϵ_1 and ϵ_2 are the amplitudes of the initial disturbance and where we have assumed the aspect ratio δ of the periodic domain of the disturbance to be order unity (see (1.6) and (1.7)).

The behaviour of $A_{n,0}$ and $A_{n,\pm 1}$ in (6.1) and (6.2) is in qualitative agreement with that of numerical solutions in §3. Figure 2 shows a quantitative comparison between the Fourier coefficients $X_{n,0}$ and $X_{n,1}$ at $t = 10.3$ obtained in §3 and those obtained by substituting $\epsilon_2 = 0.001$, $t_c = 10.3$ and $\delta = 1$ into

$$\epsilon_1^n X_{n,0}^{(0)} \sim t_c^{-1} a_{n,0}^{(0)} \mathrm{e}^{-n}, \tag{6.3}$$

$$\epsilon_1^n \epsilon_2 X_{n,1}^{(0)} \sim \tfrac{1}{4}\delta(\epsilon_2 t_c) a_{n,1}^{(0)} \mathrm{e}^{-n}. \tag{6.4}$$

The agreement is fair.

The leading-order asymptotic forms of $X_{n,0}$ and $Z_{n,0}$ for large n at $t = t_c$ are given by

$$X_{n,0} = Z_{n,0} = \mathrm{i}(2\pi)^{-1/2}(-1)^n t_c^{-1} n^{-5/2} \tag{6.5}$$

(see (4.11)). Similarly, provided that $\delta \ll 1$, the forms of $X_{n,\pm 1}$, $Y_{n,\pm 1}$ and $Z_{n,\pm 1}$ for large n at $t = t_c$ are given by

$$X_{n,\pm 1} = Z_{n,\pm 1} = \mp\tfrac{1}{4}\mathrm{i}(-1)^n C_\delta \delta(\epsilon_2 t_c) n^{-3/2}, \tag{6.6}$$

and

$$Y_{n,\pm 1} = -\tfrac{1}{4}\mathrm{i}(-1)^n C_\delta \delta^2(\epsilon_2 t_c) n^{-5/2}, \tag{6.7}$$

where $C_\delta \approx (2/\pi)^{1/2}((3/e) - 1)\left(-\frac{1}{8}\delta^2\right)$ (see (4.15) and (4.22)). Small δ corresponds to large wavelength of the initial disturbance in the spanwise direction.

Throughout the analysis in §4, we assume (1.7), i.e. $0 < \epsilon_1 \ll 1$ and $\epsilon_2 = O(\epsilon_1)$, from which we have $t_c = O(\ln \epsilon_1^{-1}) \gg 1$, so that

$$\epsilon_2 t_c \ll t_c^{-1} \ll 1. \qquad (6.8)$$

It can be seen from (6.1) that the ordering $A_{n,m} = O(\epsilon_1^{|n|} \epsilon_2^{|m|})$, on which (4.1) is based, fails at the time t_c. In the two-dimensional case, as noted by Moore (1979), the simplified equation (1.4) still remains valid at the critical time t_c provided that $O(t_c^{-1})$ is small enough, because it retains the linear term that is dominant in the full equation at that time. This discussion can also be applied to the present case, because (4.2) retains the linear term and the Fourier coefficients are small enough at $t = t_c$. More precisely, we have neglected nonlinear terms of order t_c^{-2} in the equation for $A_{n,0}$ and those of order $\epsilon_2(= \epsilon_2 t_c \times t_c^{-1})$ in the equation for $A_{n,\pm 1}$ at the critical time. In this context, we may regard the results obtained in §4 as the approximations valid when (6.8) is guaranteed. Shelley (1992) presented an example which shows that when there is no linear term, in contrast to the present problem, the application of Moore's method of expansion may result in an incorrect prediction of the form of the singularity.

From (6.1) and (6.2), it may be expected that $|A_{n,\pm 1}|$ is larger than $|A_{n,0}|$ for $n \gg O((\epsilon_2 t_c^2)^{-1})$. This range of n, however, is beyond our approximation because we have neglected the terms $a_{n,0}^{(1)}$ and $a_{n,\pm 1}^{(1)}$ in (4.5). Since $a_{n,0}^{(1)}$ in (4.10) behaves like $e^n n^{-3/2}$ (Moore 1979), (4.11) is valid only for $1 \ll n \ll t$. Moreover small but finite $\epsilon_2 \ll 1$ implies $t_c \ll (\epsilon_2 t_c^2)^{-1}$, so that $|A_{n,\pm 1}| \ll |A_{n,0}|$ for $1 \ll n \ll t_c$. Moore (1979) showed that the non-uniformity of (4.11) with respect to n arises from a factor $\exp(-n/t)$. Removing this non-uniformity by introducing a strained time, he showed that the singularity is of the same form, i.e. $n^{-5/2}$, but occurs at a slightly later time. Application of his method to the equation for $A_{n,0}^{(0)}$ would lead to the same improvement as in Moore (1979) because the equation for $A_{n,0}^{(0)}$ is equivalent to (1.4), i.e. the equation analysed by Moore. We cannot be certain regarding $A_{n,\pm 1}^{(0)}$ because we have no definite information on $a_{n,\pm 1}^{(1)}$ at present. All we can say is that, for the case of a small but finite disturbance, at the leading order of the approximation, the Fourier coefficients $A_{n,0}$ and $A_{n,\pm 1}$ behave as in (6.2) *simultaneously*.

The asymptotic analysis for $A_{0,m}$ in §5 leads to the result embodied in (5.18). In terms of the notation in §4, it can be interpreted as the y-component of $A_{0,m}$ which behaves like

$$\epsilon_2^{2k} Y_{0,2k}^{(0)}(t) \sim i \frac{1}{8\pi^{1/2}\delta} k^{-5/2} \left(\frac{\epsilon_2 \delta^2 t}{2}\right)^{2k}, \quad \epsilon_2^{2k-1} Y_{0,2k-1}^{(0)}(t) \sim 0, \qquad (6.9)$$

for large t and k. This implies that a singularity appears at a critical time $t_c^{(\text{span})} = 2/(\delta^2 \epsilon_2)$.

When $\delta = O(1)$, it is seen from $0 < \epsilon_1 \ll 1$ and $\epsilon_2 = O(\epsilon_1)$ that $O(\epsilon_2^{-1}) \gg O(\ln \epsilon_1^{-1})$, i.e. $t_c^{(\text{span})} \gg t_c$. The singularity associated with (6.9) therefore makes sense only for the case $1/\delta \to 0$. In addition, since $A[m]$ in §5 becomes of $O(1)$ at $t = t_c^{(\text{span})}$ and we have neglected nonlinear terms of $O(1)$ in the equation for $A[m]$ at that time, there is no guarantee the validity of the asymptotic analysis for $A_{0,m}$ at $t = t_c^{(\text{span})}$. However, it is expected that (6.9) well describes the behaviour of the spanwise mode at large t, for example at $t = t_c \gg 1$, because the ordering $A[m] = O(\epsilon_2^{|m|})$ still remains valid at

that time. The exponential decay of $A[m]$ with respect to m at $t = t_c$ suggests that the shape of the vortex sheet remains analytic in the spanwise direction at that time.

Sheet shape near the singularity time

Substituting (4.1) and (4.5) into (2.13) yields the following expression for the vortex sheet:

$$x(\lambda_1, \lambda_2, t) \approx \lambda_1 - 2t^{-1} \sum_{n=1}^{\infty} (\epsilon_1 \theta)^n \bar{a}_{n,0}^{(0)} \sin n(\lambda_1 + \pi)$$

$$+ \delta \epsilon_2 t \left\{ \sum_{n=0}^{\infty} (\epsilon_1 \theta)^n \bar{a}_{n,1}^{(0)} \cos n(\lambda_1 + \pi) \right\} \sin \delta \lambda_2, \tag{6.10a}$$

$$y(\lambda_1, \lambda_2, t) \approx \lambda_2 + \delta \epsilon_2 t \left\{ \sum_{n=1}^{\infty} (\epsilon_1 \theta)^n \bar{b}_{n,1}^{(0)} \sin n(\lambda_1 + \pi) \right\} \cos \delta \lambda_2, \tag{6.10b}$$

$$z(\lambda_1, \lambda_2, t) \approx -2t^{-1} \sum_{n=1}^{\infty} (\epsilon_1 \theta)^n \bar{a}_{n,0}^{(0)} \sin n(\lambda_1 + \pi)$$

$$+ \delta \epsilon_2 t \left\{ \sum_{n=0}^{\infty} (\epsilon_1 \theta)^n \bar{c}_{n,1}^{(0)} \cos n(\lambda_1 + \pi) \right\} \sin \delta \lambda_2, \tag{6.10c}$$

where $\theta \equiv \frac{1}{4} t \exp(\frac{1}{2} t + 1)$ and $\bar{a}_{n,0}^{(0)} \equiv a_{n,0}^{(0)} e^{-n}$, $\bar{a}_{n,\pm 1}^{(0)} \equiv a_{n,\pm 1}^{(0)} e^{-n}$, and so on. In deriving (6.10a–c), we have used the relations $\bar{a}_{n,0}^{(0)} = \bar{c}_{n,0}^{(0)}$, $\bar{a}_{n,1}^{(0)} = \bar{a}_{n,-1}^{(0)}$, $\bar{b}_{n,1}^{(0)} = -\bar{b}_{n,-1}^{(0)}$ and $\bar{c}_{n,1}^{(0)} = \bar{c}_{n,-1}^{(0)}$. Since we have discarded terms of second order in ϵ_2 in the above expressions, ϵ_2 must satisfy $0 < \epsilon_2 \ll \epsilon_1 \ll 1$, if the expressions are to be used for general t. In addition, the time t must be large in (6.10a–c), since we have retained only the $a^{(0)}$-term in (4.5). At the singularity time $t_c = O(\ln(\epsilon_1^{-1}))$ at which $\epsilon_1 \theta = 1$, the expressions can make sense also for $0 < \epsilon_2 = O(\epsilon_1) \ll 1$ provided that $t_c^{-1} \ll 1$ and $\epsilon_2 t_c^2 \ll 1$, because $X_{n,0}$ and $Z_{n,0}$ are $O(t_c^{-1})$ and $X_{n,\pm 1}$, $Y_{n,\pm 1}$ and $Z_{n,\pm 1}$ are $O(\epsilon_2 t_c)$ in agreement with (4.6). Note also that (6.10a–c) are valid only for $t \gg 1$ and $1 \leqslant n \ll t$, as discussed previously in this section.

In this subsection, we consider the sheet shape near the singularity time and present a few possible interpretations of (6.10a–c).

Interpretation (a)

We first note that $\bar{a}_{n,0}^{(0)}$, $\bar{b}_{n,1}^{(0)}$ and $\bar{c}_{n,0}^{(0)}$ behave like $n^{-5/2}$ at large n, and $\bar{a}_{n,1}^{(0)}$ and $\bar{c}_{n,1}^{(0)}$ behave like $n^{-3/2}$ at t_c, and each sum in (6.10a–c) with respect to n therefore is singular at $\lambda_1 = (2k + 1)\pi$, where k is an integer. One possible and straightforward interpretation compatible with these facts may be to construe that the shape of the sheet is singular at $\lambda_1 = (2k + 1)\pi$. If this is the case, the singularity is distributed along vortex lines given by

$$\left. \begin{aligned} x(\lambda_2) &= (2k + 1)\pi + \delta \epsilon_2 t_c \sum_{n=0}^{\infty} \bar{a}_{n,1}^{(0)} \sin \delta \lambda_2 \\ y(\lambda_2) &= \lambda_2, \\ z(\lambda_2) &= \delta \epsilon_2 t_c \sum_{n=0}^{\infty} \bar{c}_{n,1}^{(0)} \sin \delta \lambda_2 \end{aligned} \right\} \quad (k = 0, \pm 1, \pm 2, \cdots), \tag{6.11}$$

which is obtained by substituting $\lambda_1 = (2k + 1)\pi$ into (6.10a–c). Each of the vortex lines is on a plane with the slope

$$\Theta \equiv \frac{z(\lambda_2)}{x(\lambda_2) - (2k + 1)\pi} = \frac{\displaystyle\sum_{n=0}^{\infty} \bar{c}_{n,1}^{(0)}}{\displaystyle\sum_{n=0}^{\infty} \bar{a}_{n,1}^{(0)}}. \tag{6.12}$$

This slope depends only on δ. For example, it was obtained numerically from (4.14a,b) that $\Theta = -1.24 \times 10^3, -17.9$ and -0.32 for $\delta = 0.1, 1$ and 10, respectively.

Since (6.10a–c) are valid only for $1 \leqslant n \ll t_c$ and $|A_{n,\pm 1}| \ll |A_{n,0}|$ for this range of n, we may understand (6.10a–c) to show that the sheet shape at t_c is dominated by $A_{n,0}$ and the three-dimensional motion results in the same curvature singularity as in two dimensions at the leading order of the present approximation. Thus the effect of the three-dimensional correction associated with $A_{n,\pm 1}$ on the sheet profile may be regarded as small. However, it may play a key role in the vector W in (2.4), because (6.10a–c) give

$$W = \begin{pmatrix} 0 \\ 1 \\ 0 \end{pmatrix} + \delta^2 \epsilon_2 t_c \begin{pmatrix} \displaystyle\sum_{n=0}^{\infty} \bar{a}_{n,1}^{(0)} \cos n(\lambda_1 + \pi) \cos \delta\lambda_2 \\ -\displaystyle\sum_{n=0}^{\infty} \bar{b}_{n,1}^{(0)} \sin n(\lambda_1 + \pi) \sin \delta\lambda_2 \\ \displaystyle\sum_{n=0}^{\infty} \bar{c}_{n,1}^{(0)} \cos n(\lambda_1 + \pi) \cos \delta\lambda_2 \end{pmatrix} + O(\epsilon_2), \tag{6.13}$$

at $t = t_c$, where the second term is due to the effect of three-dimensionality or vortex stretching. The length of W represents the vortex stretching and is given by

$$|W| = 1 - \delta^2 \epsilon_2 t_c \sum_{n=0}^{\infty} \bar{b}_{n,1}^{(0)} \sin n(\lambda_1 + \pi) \sin \delta\lambda_2 + O(\epsilon_2).$$

The fact that $|W| = 1$ at $\lambda_1 = (2k + 1)\pi$ implies that there is no stretching in order $\epsilon_2 t_c$ on the curve given by (6.11).

From (6.13) and (2.5) the vorticity density vector Ω may be written as

$$\Omega = \begin{pmatrix} 0 \\ 1 \\ 0 \end{pmatrix} + \begin{pmatrix} \delta^2 \epsilon_2 t_c \displaystyle\sum_{n=0}^{\infty} \bar{a}_{n,1}^{(0)} \cos n(\lambda_1 + \pi) \cos \delta\lambda_2 \\ t_c^{-1} \displaystyle\sum_{n=1}^{\infty} \bar{a}_{n,0}^{(0)} n \cos n(\lambda_1 + \pi) \\ \delta^2 \epsilon_2 t_c \displaystyle\sum_{n=0}^{\infty} \bar{c}_{n,1}^{(0)} \cos n(\lambda_1 + \pi) \cos \delta\lambda_2 \end{pmatrix} + \begin{pmatrix} O(\epsilon_2) \\ O(t_c^{-2}) \\ O(\epsilon_2) \end{pmatrix},$$

at $t = t_c$, in which we have retained only the dominant term in each element. The amplitude of the vorticity density $|\Omega|$ is then

$$|\Omega| = 1 + t_c^{-1} \sum_{n=1}^{\infty} \bar{a}_{n,0}^{(0)} n \cos n(\lambda_1 + \pi) + O(t_c^{-2}). \tag{6.14}$$

Equations (6.13) and (6.14) with the above interpretation regarding the singularity

location suggest that the x- and z-components of W as well as $|\Omega|$ have cusp singularities at $\lambda_1 = (2k + 1)\pi$. Since $\bar{a}_{n,0}^{(0)}$ can be determined by the dynamics of the vortex sheet in two-dimensional flow, it is clear from (6.14) that the singularity distribution of the vorticity density is dominated by two-dimensional dynamics, i.e. by the concentration of vorticity associated with Kelvin–Helmholtz instability.

Interpretation (b)

Interpretations different from (a) are also possible. For example, the following interpretation based on the idea of strained coordinates is also compatible with (6.10a–c) as well as (6.5)–(6.7). An illustrative example to make the idea clear is

$$\sin n(\lambda_1 + \epsilon) \sim \sin n\lambda_1 + n\epsilon \cos n\lambda_1 \quad \text{as} \quad \epsilon \to 0, \tag{6.15}$$

where a slight distortion ϵ results in a term proportional to n on the right-hand side. This expansion is valid only for $\epsilon \ll 1$ and $n \ll \epsilon^{-1}$. With (6.15) in mind, we rewrite (6.10a) as

$$x(\lambda_1, \lambda_2, t) \approx \lambda_1 - 2t^{-1} \sum_{n=1}^{\infty} (\epsilon_1 \theta)^n \left\{ \bar{a}_{n,0}^{(0)} \sin n(\lambda_1 + \pi) - \tfrac{1}{2}\delta\epsilon_2 t^2 \bar{a}_{n,1}^{(0)} \sin \delta\lambda_2 \cos n(\lambda_1 + \pi) \right\}. \tag{6.16}$$

Since $\bar{a}_{n,0}^{(0)} \sim (2\pi)^{-1/2} n^{-5/2}$ and $\bar{a}_{n,1}^{(0)} \sim C_\delta n^{-3/2}$ for large n (see (4.10) and (4.15)), we have $\bar{a}_{n,1}^{(0)}/\bar{a}_{n,0}^{(0)} \sim (2\pi)^{-1/2} C_\delta n$ for large n. Let $\alpha(n)$ be defined by $n\alpha(n) \equiv \bar{a}_{n,1}^{(0)}/\bar{a}_{n,0}^{(0)}$, then utilizing (6.15) to (6.16) gives

$$x(\lambda_1, \lambda_2, t) \approx \lambda_1 - 2t^{-1} \sum_{n=1}^{\infty} (\epsilon_1 \theta)^n \bar{a}_{n,0}^{(0)} \sin n\{\lambda_1 + \pi - \tfrac{1}{2}\alpha(n)\delta\epsilon_2 t^2 \sin \delta\lambda_2\}, \tag{6.17}$$

where $\alpha(n) \sim (2\pi)^{-1/2} C_\delta$ for large n. Similarly, we have from (6.10c)

$$z(\lambda_1, \lambda_2, t) \approx -2t^{-1} \sum_{n=1}^{\infty} (\epsilon_1 \theta)^n \bar{a}_{n,0}^{(0)} \sin n\{\lambda_1 + \pi - \tfrac{1}{2}\beta(n)\delta\epsilon_2 t^2 \sin \delta\lambda_2\}, \tag{6.18}$$

where $n\beta(n) \equiv \bar{c}_{n,1}^{(0)}/\bar{a}_{n,0}^{(0)} \sim (2\pi)^{-1/2} C_\delta n$ for large n and we have neglected a term associated with $\bar{c}_{0,1}^{(0)}$ which is irrelevant to the singularity analysis. Since (1.7) implies $\epsilon_2 t^2 \ll 1$ and $t \ll (\epsilon_2 t^2)^{-1}$, (6.17) and (6.18) can be valid for $1 \leqslant n \ll t$, in the same sense as (6.10a) and (6.10c).

Since $\alpha(n) = \beta(n) \sim (2\pi)^{-1/2} C_\delta$ for large $n(\gg \delta = O(1))$, which is justified by (4.14b) and (4.15), (6.17) and (6.18) are compatible with the interpretation that the singularity of the same form as the two-dimensional curvature singularity appears at t_c and it is distributed along the curves given by

$$\lambda_1 = (2k + 1)\pi + \tfrac{1}{2}(2\pi)^{-1/2} C_\delta \delta\epsilon_2 t_c^2 \sin \delta\lambda_2, \tag{6.19}$$

where $k = 0, \pm 1, \pm 2, \cdots$. In contrast to the interpretation (a), these singularity curves are then different from vortex lines satisfying $\lambda_1 =$ constant (these cannot occur in two dimensions). Equation (6.19) means that the λ_1(streamwise coordinate)-value of the singularity curves varies with λ_2(spanwise coordinate) by an amount of $O(\epsilon_2 t_c^2)$. If this is the reason for the $n^{-3/2}$ behaviour of $A_{n,\pm 1}$, then it is suggested from (6.17) and (6.18) that at time t_c, $A_{n,\pm 2} = O(\epsilon_2^2 t_c^3) \propto n^{-1/2}$ for large n, $A_{n,\pm 3} = O(\epsilon_2^3 t_c^5) \propto n^{1/2}$ for large n, and so on. The data in figure 2 seem to be too limited to check this behaviour. Moore (1979) showed rigorously that the non-uniformity in the perturbation expansion for

large n results in the $n^{-3/2}$ behaviour of $\bar{a}_{n,0}^{(1)}$ for large n, and such a non-uniformity can be removed by introducing the strained time. The ordering of Fourier coefficients at t_c, i.e., $A_{n,\pm 2} = O(\epsilon_2^2 t_c^3)$ and $A_{n,\pm 3} = O(\epsilon_2^3 t_c^5)$ at t_c is consistent with (4.5).

It is shown from (6.17) and (6.18) that at time t_c,

$$W_x = \delta^2 \epsilon_2 t_c \sum_{n=1}^{\infty} \bar{a}_{n,1}^{(0)} \cos n\{\lambda_1 + \pi - \tfrac{1}{2}\alpha(n)\delta\epsilon_2 t_c^2 \sin \delta\lambda_2\} \cos \delta\lambda_2 + O(\epsilon_2), \quad (6.20)$$

$$W_z = \delta^2 \epsilon_2 t_c \sum_{n=1}^{\infty} \bar{c}_{n,1}^{(0)} \cos n\{\lambda_1 + \pi - \tfrac{1}{2}\beta(n)\delta\epsilon_2 t_c^2 \sin \delta\lambda_2\} \cos \delta\lambda_2 + O(\epsilon_2), \quad (6.21)$$

and

$$|\Omega| = 1 + t_c^{-1} \sum_{n=1}^{\infty} \bar{a}_{n,0}^{(0)} n \cos n\{\lambda_1 + \pi - \tfrac{1}{2}\alpha(n)\delta\epsilon_2 t_c^2 \sin \delta\lambda_2\} + O(t_c^{-2}). \quad (6.22)$$

These with the interpretation based on (6.19) suggest that W_x, W_z and $|\Omega|$ have cusp singularities along the curve defined by (6.19) provided that $\delta = O(1)$. These facts coincide with those obtained in interpretation (a) except for the location of the singularity.

By the way, one might consider that the $n^{-3/2}$ behaviour of $A_{n,\pm 1}$ for large n would result if the singularity time varies with the spanwise coordinate λ_2. (This possibility was commented on by a referee.) An expansion similar to

$$\sin n\lambda_1 \exp(\epsilon n \cos \delta\lambda_2) \sim \sin n\lambda_1 + \epsilon n \cos \delta\lambda_2 \sin n\lambda_1 \quad \text{as} \quad \epsilon \to 0, \quad (6.23)$$

which is consistent with $A_{-n,-m} = -A_{n,m}$, certainly explains the $n^{-3/2}$ behaviour of $A_{n,\pm 1}$ and leads to this conjecture. However, this possibility can be excluded at the leading-order approximation for the present problem, because (6.23) is incompatible with $\bar{a}_{n,1}^{(0)} = \bar{a}_{n,-1}^{(0)}$ and $\bar{c}_{n,1}^{(0)} = \bar{c}_{n,-1}^{(0)}$ which come from the initial condition (2.12) and the evolution equation obtained in §4.

The main difference between interpretations (a) and (b) lies in the location of the singularity. In interpretation (a), the singularity is distributed along *a vortex line*, while, in interpretation (b), it is distributed along a curve defined by (6.19) for $\delta = O(1)$, which is *not* a vortex line. On the other hand, irrespectively of the interpretations, the form and the appearance time of the singularity in the three-dimensional motion are the same as those in two dimensions at the leading-order approximation for the present problem. In both interpretations, it is seen that, reflecting three-dimensionality, in contrast to two dimensions where W given by (2.4) is kept constant, x- and z-components of W form cusp singularities in three dimensions.

The full determination of the location as well as the form and the appearance time of the singularity would require the full asymptotics of $A_{n,m}$ for large n and m. The results in the present paper are clearly insufficient for the full determination; they do not rule out possibilities other than interpretations (a) and (b). It would be interesting to investigate numerically the nature of the singularity in three dimensions, as in the two-dimensional computation by Krasny(1986) and Shelley(1992). It would be also interesting to check numerically the λ_2-dependence (or independence) of the singularity time for various initial conditions. A numerical study in such a direction is now under way.

REFERENCES

BATCHELOR, G. K. 1967 *An Introduction to Fluid Dynamics*. Cambridge University Press.

BAKER, G. R., MEIRON, D. I. & ORSZAG, S. A. 1984 Boundary integral methods for axisymmetric and three-dimensional Rayleigh-Taylor instability problems. *Physica* D **12**, 19–31.

BIRKHOFF, G. 1962 Helmholtz and Taylor instability. In *Proc. Symp. Appl. Maths* XIII. pp. 55–76. AMS.

CAFLISCH, R. E. 1989 Mathematical analysis of vortex dynamics. In *Proc. Workshop on Mathematical Aspects of Vortex Dynamics*. (ed. R. E. Caflisch), pp. 1–24. SIAM.

ISHIHARA, T. & KANEDA, Y. 1994 Spontaneous singularity formation in the shape of vortex sheet in three-dimensional flow. *J. Phys. Soc. Japan*. **63**, 388–392.

KANEDA, Y. 1990 A representation of the motion of a vortex sheet in a three-dimensional flow. *Phys. Fluids* A **2**, 458–461. (Also presented at the meeting held in July, 1989 at the Research Institute of Mathematical Science, Kyoto University.)

KRASNY, R. 1986 A study of singularity formation in a vortex sheet by the point-vortex approximation. *J. Fluid Mech.* **167**, 65–93.

KRASNY, R. 1990 Computing vortex sheet motion. In *Proc. Intl Congr. of Mathematicians* II, pp. 1573–1583. Springer.

MEIRON, D. I., BAKER, G. R. & ORSZAG S. A. 1982 Analytical structure of vortex sheet dynamics. Part 1. Kelvin-Helmholtz instability. *J. Fluid Mech.* **114**, 283–298.

MOORE, D. W. 1979 The spontaneous appearance of a singularity in the shape of an evolving vortex sheet. *Proc. R. Soc. Lond.* A **365**, 105–119.

ROSENHEAD, L. 1931 The formation of vortices from a surface of discontinuity. *Proc. R. Soc. Lond.* A **134**, 170–191.

ROTT, N. 1956 Diffraction of a weak shock with vortex generation. *J. Fluid Mech.* **1**, 111–128.

SHELLEY, M. 1992 A study of singularity formation in vortex-sheet motion by a spectrally accurate vortex method. *J. Fluid Mech.* **244**, 493–526.